



U-Pb zircon dates for rhyolite and sandstone of Cadwallader terrane, lower Chilcotin River area, south-central British Columbia

Paul Schiarizza^{1, a}, and Richard M. Friedman²

¹ British Columbia Geological Survey, Ministry of Energy, Mines and Low Carbon Innovation, 300-865 Hornby Street, Vancouver, BC, V6Z 2G3

² Retired, formerly at Pacific Centre for Isotopic and Geochemical Research, Department of Earth, Ocean and Atmospheric Sciences, The University of British Columbia, Vancouver, BC, V6T 1Z4

^a corresponding author: Paul.Schiarizza@gov.bc.ca

Recommended citation: Schiarizza, P., and Friedman, R.M., 2023. U-Pb zircon dates for rhyolite and sandstone of Cadwallader terrane, lower Chilcotin River area, south-central British Columbia. In: Geological Fieldwork 2022, British Columbia Ministry of Energy, Mines and Low Carbon Innovation, British Columbia Geological Survey Paper 2023-01, pp. 65-84.

Abstract

Cadwallader terrane, exposed in a structural window beneath overthrust Cache Creek terrane along the Chilcotin River, 50 km southwest of Williams Lake, comprises: 1) basalt, rhyolite and tonalite of the Wineglass assemblage (Late Permian); 2) conglomerates and sandstones (Tyaughton Formation, Late Triassic) that rest unconformably above the Wineglass assemblage; and 3) siltstones and sandstones (Ladner Group, Early and Middle Jurassic) that are disconformably above the Tyaughton Formation. Rhyolite from near the top of the Wineglass assemblage, dated using the U-Pb zircon chemical abrasion thermal ionization mass spectrometry method (CA-TIMS), crystallized at 260.8 ± 0.3 Ma. Detrital zircons from red sandstone in the lower part of the Tyaughton Formation, dated with Laser Ablation Inductively Coupled Plasma Mass Spectrometry (LA-ICP-MS), include a population of Late Permian to Middle Triassic grains, probably derived from the underlying Wineglass assemblage and/or related rocks, and a population of Late Triassic grains that are inferred to have been derived from Late Triassic volcanic and plutonic rocks exposed elsewhere in Cadwallader terrane. Green sandstone from a higher stratigraphic level in the Tyaughton Formation contains only Late Triassic zircons, and these have a range that is very similar to that of detrital zircons analyzed from a sample of Hurley Formation (Late Triassic) in a separate fault panel north of the Chilcotin River window. The Permian to Jurassic rocks exposed in the Chilcotin River window represent the Tyaughton Creek facies of Cadwallader terrane, which contrasts with other parts of the terrane (Camelsfoot facies) represented mainly by the Pioneer and Hurley formations of the Cadwallader Group (Middle to Late Triassic). The Permian to Jurassic rocks of the Tyaughton Creek facies correlate with rocks in central British Columbia (Sitlika assemblage) and northern British Columbia (Kutcho assemblage and overlying rocks), forming a fragmented belt that can be traced the full south to north length of British Columbia.

Keywords: Cadwallader terrane, Wineglass assemblage, Tyaughton Formation, Hurley Formation, Late Permian, Late Triassic, U-Pb, zircon, CA-TIMS, LA-ICP-MS

1. Introduction

Read (1992, 1993) identified Late Permian volcanic and intrusive rocks along the lower reaches of the Chilcotin River southwest of Williams Lake. These rocks were in part mapped by Schiarizza (2013), who referred to them as the Wineglass assemblage and correlated them with the Sitlika and Kutcho assemblages of central and northern British Columbia. Schiarizza (2013) also correlated undated conglomerates and sandstones that rest unconformably above the Permian rocks with the Tyaughton Formation (Late Triassic) of Cadwallader terrane, thus inferring that the Wineglass assemblage is also part of that terrane. Four samples collected during this mapping were submitted for U-Pb zircon isotopic dating at the Pacific Centre for Isotopic and Geochemical Research (PCIGR), Department of Earth, Ocean and Atmospheric Sciences, the University of British Columbia. Herein we present the geochronologic data and age interpretations for these samples. One sample of rhyolite was dated using the U-Pb zircon chemical abrasion

thermal ionization mass spectrometry method (CA-TIMS), confirming the Late Permian age for at least the upper part of the Wineglass assemblage. The other three samples are sandstones, submitted for U-Pb detrital zircon analysis using Laser Ablation Inductively Coupled Plasma Mass Spectrometry (LA-ICP-MS). Two sandstone samples are from the sedimentary succession that is unconformably above the Wineglass assemblage, and the data corroborate its correlation with the Tyaughton Formation. The third sandstone sample is from the Hurley Formation in an adjacent fault panel; these zircons are very similar to those from the Tyaughton Formation, confirming that the Hurley and Tyaughton formations are part of the same terrane.

2. Setting

The lower Chilcotin River area is on the Fraser Plateau, along and west of the Fraser River, within the traditional territories of the Tsilhqot'in and Secwepemc First Nations (Figs. 1, 2). It is underlain, in large part, by late Paleozoic and early Mesozoic

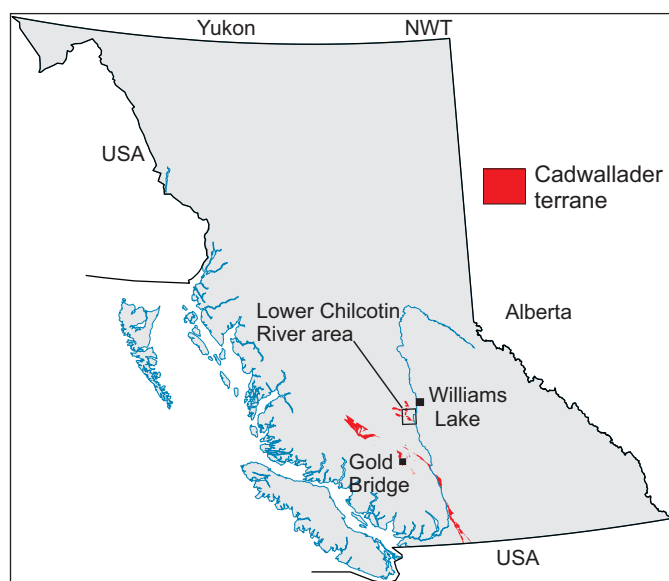


Fig. 1. Location of the lower Chilcotin River area and distribution of Cadwallader terrane (after Schiarizza, 2013) in southern British Columbia.

rocks assigned to Cache Creek terrane, Cadwallader terrane, and Thaddeus assemblage, the latter comprising Carboniferous greenstone and limestone of uncertain correlation or terrane affinity (Read, 1993). These units are separated from one another by thrust faults, of uncertain Middle Jurassic to mid-Cretaceous age, that are commonly marked by serpentinite melange (Fig. 2; Read, 1993). Younger rocks exposed in the area include small Middle to Late Jurassic diorite and quartz diorite intrusions, Eocene volcanic and sedimentary rocks, and flat-lying Neogene basalts of the Chilcotin Group.

The Cache Creek complex (Cache Creek terrane) is subdivided into three composite units: one comprising chert, siliceous phyllite, and limestone; another of basalt and limestone; and a third of mainly siltstone and sandstone (Fig. 2). Biochronologic data come mainly from the chert-siliceous phyllite-limestone unit, which has yielded Early Permian, Middle Triassic, and Late Triassic radiolarians (Cordey and Read, 1992). A large body of diorite and gabbro that is also included in Cache Creek terrane (Fig. 2) has yielded a U-Pb zircon age of 241.5 ± 0.5 Ma (Middle Triassic; Mahoney et al., 2013).

Cadwallader terrane is represented, in part, by Upper Triassic sandstone, conglomerate and limestone of the Hurley Formation, which occurs west of Cache Creek terrane along and north of the Chilcotin River, and also forms a folded thrust panel that encompasses Bald Mountain (Fig. 2). A much different group of rocks (Late Permian to Early Jurassic) that are also part of Cadwallader terrane are exposed in a structural window beneath Cache Creek terrane (Chilcotin River window) southeast of the Hurley exposures (Fig. 2).

2.1. Geology of the Chilcotin River window

The Chilcotin River window, 22 km long and up to 6.5 km wide, is an inlier of Late Permian to Early Jurassic rocks that

are structurally beneath rocks of Cache Creek terrane along and southwest of the Chilcotin River (Fig. 2). It is mainly underlain by Late Permian volcanic and intrusive rocks assigned to the Wineglass assemblage, but also includes conglomerates and sandstones that are unconformably above the Permian rocks, and a younger unit of finer grained siliciclastic rocks that contain Early Jurassic fossils. Schiarizza (2013) correlated the conglomerate-sandstone unit with the Tyaughton Formation (Late Triassic), and assigned the overlying Jurassic rocks to the Ladner Group.

The Wineglass assemblage is in large part represented by the Wineglass pluton, a body of tonalite, quartz diorite and granodiorite that has yielded U-Pb crystallization ages of 258 ± 5 Ma (Friedman and van der Heyden, 1992) and 254 ± 1.2 Ma (Read, 1993). Volcanic and volcanoclastic rocks of the assemblage are best exposed on the southwest margin of the Wineglass pluton (Fig. 3) where they were mapped and subdivided into two units by Schiarizza (2013). The oldest unit (Wv1) is mainly basalt and basalt-derived chlorite schist, but also includes narrow units of felsic volcanic rock (dikes, sills, or flows) and small bodies of diorite. These rocks are overlain by a more heterogeneous unit (Wv2) that includes basalt and pillowed basalt, rhyolite and dacite flows, and volcanoclastic rocks containing quartz, feldspar and felsic to mafic volcanic lithic fragments. Read (1993) reported a U-Pb zircon age of 259 ± 2 Ma from dacite of unit Wv2. This Late Permian age is confirmed by the CA-TIMS age (260.8 ± 0.3 Ma) reported here.

The Tyaughton Formation comprises a southwest-dipping succession of siliciclastic sedimentary rocks that rests unconformably above the Wineglass assemblage near the southwest margin of the Chilcotin River window (Figs. 2, 3). It includes a basal unit of mainly red pebble conglomerates, and an overlying unit of massive, blue-green to olive green sandstones (Schiarizza, 2013). The conglomerates of the basal unit consist mainly of felsic volcanic fragments, but also include clasts of tonalite, mafic volcanic rock, chert, and microdiorite.

The youngest rocks exposed in the Chilcotin River window are assigned to the Ladner Group (Early to Middle Jurassic). They comprise grey, thin-bedded siltstones and fine- to medium-grained sandstones that overlie the Tyaughton Formation across a sharp, probably disconformable contact (Fig. 3). Hickson (1990) reported that fossils collected from the lower part of this unit are Early Jurassic (Toarcian).

3. CA-TIMS geochronology

Here we present U-Pb zircon isotopic dating results obtained by the chemical abrasion thermal ionization mass spectrometry method (CA-TIMS) for one rhyolite sample collected from the Wineglass assemblage.

3.1. Analytical procedures

CA-TIMS procedures described here are modified from Mundil et al. (2004), Mattinson (2005) and Scoates and Friedman (2008). After rock samples underwent standard mineral separation procedures, zircons were handpicked

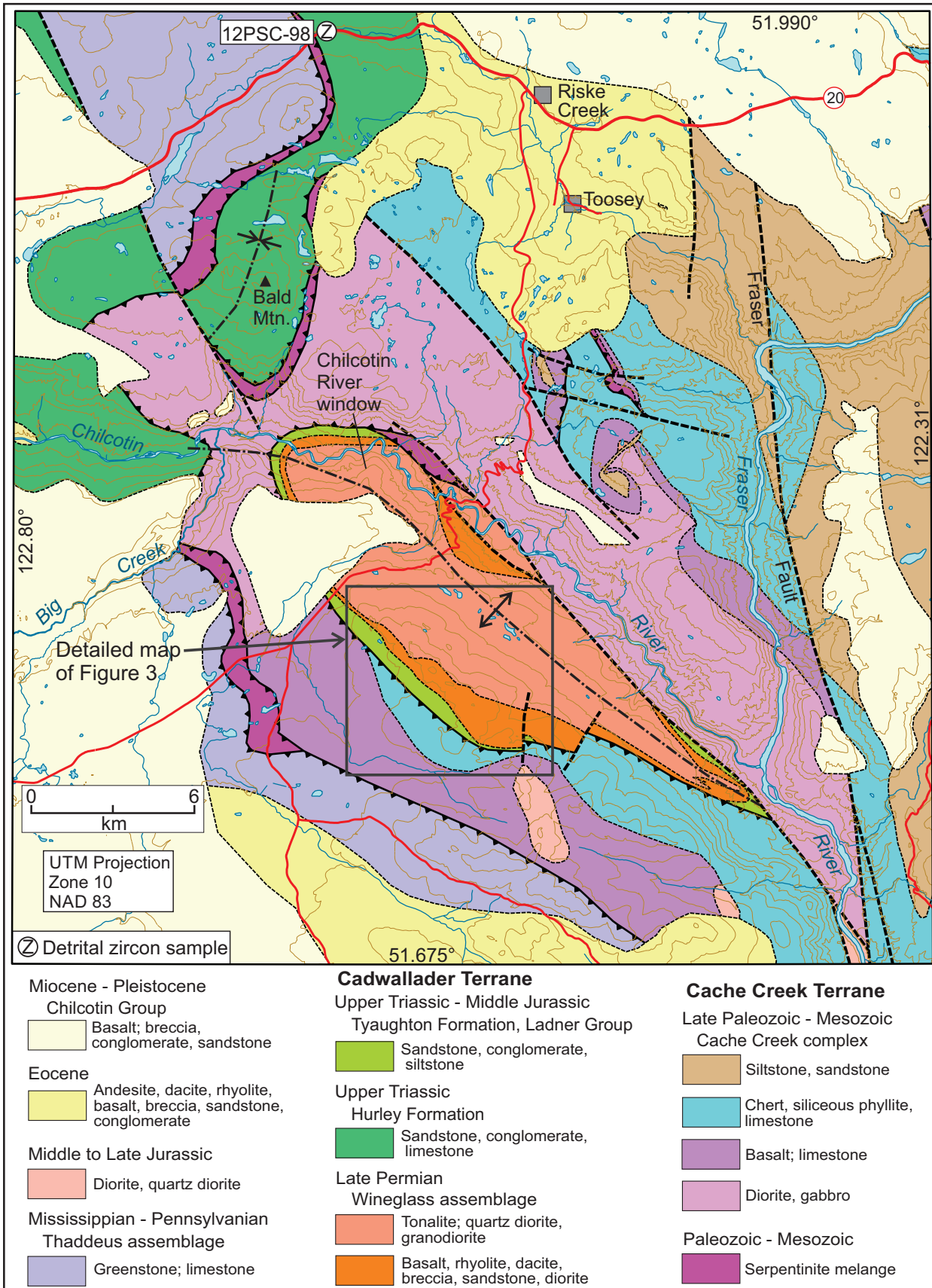


Fig. 2. Geology of the lower Chilcotin River area, after Tipper (1978), Read (1993), Mihalynuk and Harker (2007), Mahoney et al. (2013), and Schiarizza (2013).

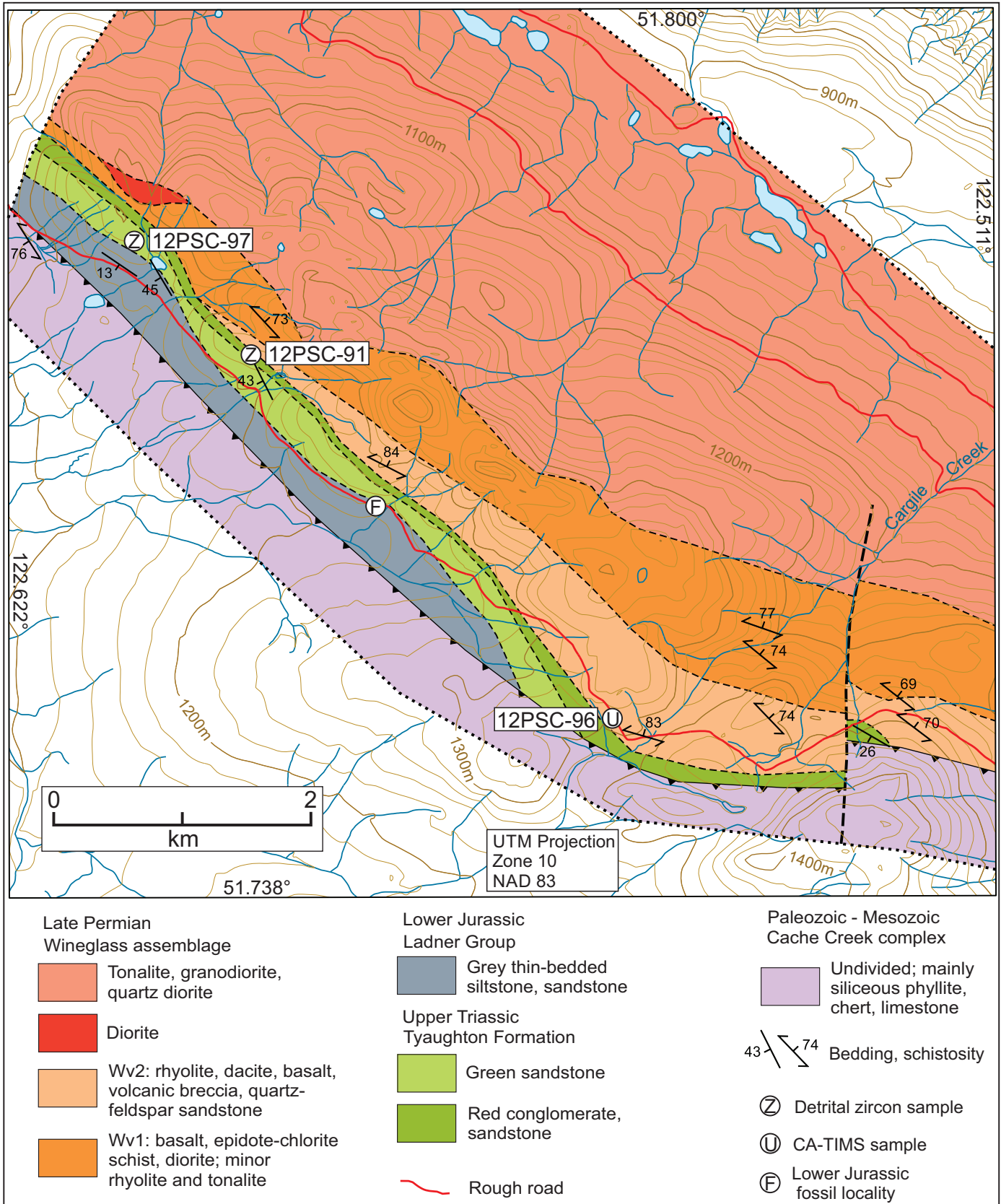


Fig. 3. Geology of the southwestern part of the Chilcotin River window, after Schiarizza (2013).

in alcohol. The clearest, crack- and inclusion-free grains were selected, photographed, and then annealed in quartz glass crucibles at 900°C for 60 hours. Annealed grains were transferred into 3.5 mL PFA screwtop beakers, ultrapure HF (up to 50% strength, 500 μ L) and HNO₃ (up to 14 N, 50 μ L) were added and caps were closed finger tight. The beakers were placed in 125 mL PTFE liners (up to four per liner) and about 2 mL HF and 0.2 mL HNO₃, of the same strength as the acid in the beakers containing the samples, were added to the liners. The liners were then slid into stainless steel Parr™ high-pressure dissolution devices, which were sealed and brought to a maximum of 200°C for 8-16 hours (typically 175°C for 12 hours). Beakers were removed from the liners and zircon was separated from the leachate. Zircons were rinsed with >18 M Ω .cm water and subboiled acetone. Then 2 mL of subboiled 6N HCl was added and beakers were set on a hotplate at 80-130°C for 30 minutes and again rinsed with water and acetone. Masses were estimated from the dimensions (volumes) of grains. Single grains were transferred into clean 300 μ L PFA microcapsules (crucibles), and 50 μ L 50% HF and 5 μ L 14 N HNO₃ were added. Each was spiked with a ²³³⁻²³⁵U-²⁰⁵Pb tracer solution (EARTHTIME ET535), capped and again placed in a Parr liner (8-15 microcapsules per liner). HF and nitric acids, in a 10:1 ratio, were added to the liner, which was then placed in a Parr high-pressure device and dissolution was achieved at 240°C for 40 hours. The resulting solutions were dried on a hotplate at 130°C, 50 μ L 6N HCl was added to microcapsules and fluorides were dissolved in high-pressure Parr devices for 12 hours at 210°C. HCl solutions were transferred into clean 7 mL PFA beakers and dried with 2 μ L of 0.5 N H₃PO₄. Samples were loaded onto degassed, zone-refined Re filaments in 2 μ L of silicic acid emitter (Gerstenberger and Haase, 1997).

Isotopic ratios were measured by a modified single collector

VG-54R or 354S (with Sector 54 electronics) thermal ionization mass spectrometer equipped with analogue Daly photomultipliers. Analytical blanks were 0.2 pg for U and up to 1 pg for Pb. U fractionation was determined directly on individual runs using the EARTHTIME ET535 mixed ²³³⁻²³⁵U-²⁰⁵Pb isotopic tracer. Pb isotopic ratios were corrected for fractionation of 0.25 \pm 0.03%/amu, based on replicate analyses of NBS-982 reference material and the values recommended by Thirlwall (2000). Data reduction employed the Excel-based program of Schmitz and Schoene (2007). Standard concordia diagrams were constructed and weighted averages calculated with Isoplot (Ludwig, 2003). Interpreted ages for all samples are based on weighted ²⁰⁶Pb/²³⁸U dates reported at the 2 sigma confidence level in the three error, $\pm X (Y) [Z]$ format of Schoene et al. (2006), where X includes internal errors only, largely comprised of analytical (counting statistics), mass fractionation and common lead composition uncertainties. The (Y) error includes X plus isotopic tracer calibration uncertainty and [Z] additionally includes uranium decay constant errors. Isotopic dates are calculated with the decay constants $\lambda_{U238}=1.55125E^{-10}$ and $\lambda_{U235}=9.8485E^{-10}$ (Jaffey et al., 1971). EARTHTIME U-Pb synthetic solutions were analyzed on an on-going basis to monitor the accuracy of results.

3.2. Sample 12PSC-96, rhyolite, Wineglass assemblage

Sample 12PSC-96 was collected from the upper part of the upper volcanic unit of the Wineglass assemblage, about 75 m northeast of the (unexposed) contact with the overlying Tyaughton Formation (Figs. 3, 4; 530786E, 5733372N, UTM Zone 10, NAD83). It is a pale green to grey metarhyolite with abundant 1-2 mm plagioclase and quartz phenocrysts in a very fine-grained groundmass of mainly quartz, feldspar and secondary sericite (Fig. 5).

Four of the six zircon grains analyzed (Table 1) are mutually

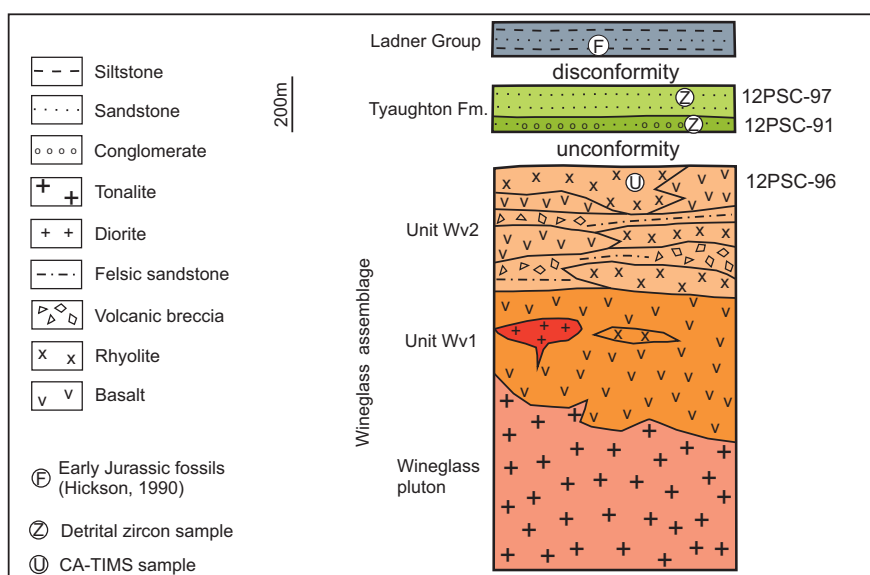


Fig. 4. Schematic stratigraphy of the Wineglass assemblage and overlying Tyaughton Formation and Ladner Group, showing stratigraphic context of geochronology samples. Vertical scale very approximate, based on bedding dips and mapped contacts of Tyaughton Formation.



Fig. 5. Quartz and plagioclase-phyric metarhyolite, Wineglass assemblage, sample site 12PSC-96.

overlapping on or near concordia, with a weighted mean $^{206}\text{Pb}/^{238}\text{U}$ date of 260.8 ± 0.3 (0.4) [0.5] Ma (MSWD=1.04), interpreted as the crystallization age of the rhyolite (Fig. 6). The other two grains give slightly younger dates (259.86 and 259.68 Ma), possibly due to minor Pb loss.

4. Detrital zircon geochronology

Here we present the results from isotopic analyses of detrital zircons extracted from three samples, two from the Tyaughton Formation where it overlies the Wineglass assemblage, and one from the Hurley Formation in an adjacent fault panel.

4.1. Analytical procedures

Zircons were analyzed using laser ablation (LA) ICP-MS methods, as described by Tafti et al. (2009). Instrumentation comprised a New Wave UP-213 laser ablation system and a ThermoFinnigan Element2 single collector, double-focusing, magnetic sector ICP-MS. All zircons greater than about 50 microns in diameter were picked from the mineral separates and mounted in an epoxy puck along with several grains of the Plešovice (337.13 ± 0.13 Ma, Sláma et al., 2007) and Temora2 (416.78 ± 0.33 Ma) zircon standards, and brought to a very high polish. The surface of the mount was washed for 10 minutes with dilute nitric acid and rinsed in ultraclean water before analysis. The highest quality portions of each grain, free of alteration, inclusions, or possible inherited cores, were selected for analysis. Line scans rather than spot analyses were employed in order to minimize elemental fractionation during the analyses. A laser power level of 38% was used, with a spot size of 30 micrometres. Backgrounds were measured with the laser shutter closed for ten seconds, followed by data collection with the laser firing for approximately 35 seconds. The time-integrated signals were analyzed using GLITTER software (Griffin et al., 2008), which automatically subtracts background

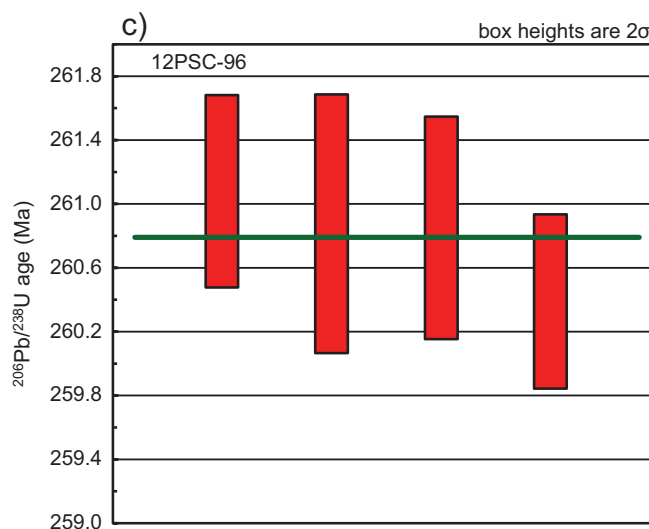
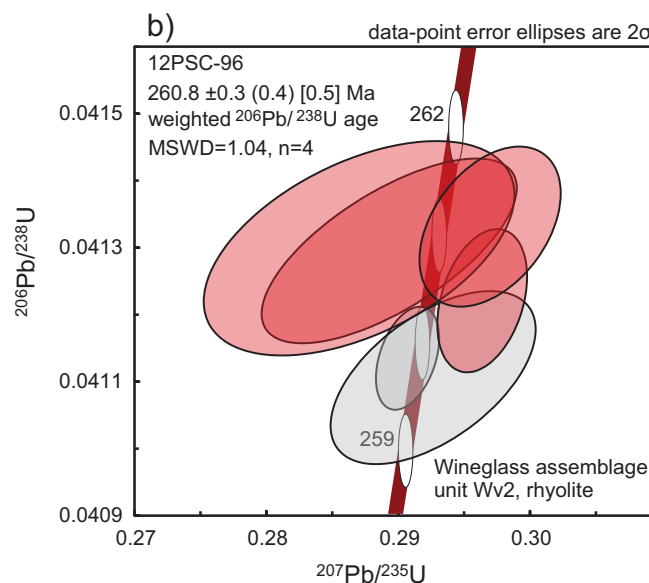
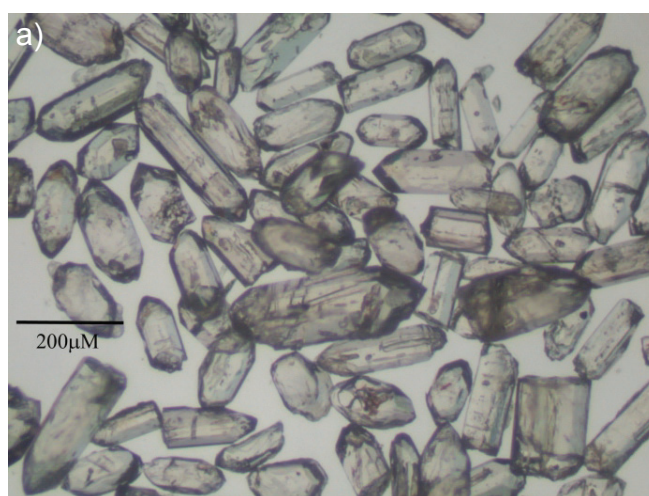


Fig. 6. U-Pb data for zircons from sample 12PSC-96. **a)** Photomicrograph of zircons. **b)** Concordia plot. **c)** $^{206}\text{Pb}/^{238}\text{U}$ ages and calculated weighted mean age, based on four of the six analyses.

Table 1. Zircon U-Th-Pb CA-TIMS analytical results for sample 12PSC-96, Wineglass assemblage rhyolite.

Sample	Compositional Parameters										Radiogenic Isotope Ratios						Isotopic Ages						
	Wt.	U	Th	Pb	$^{206}\text{Pb}^*$	mol %	Pb*	^{206}Pb	^{208}Pb	^{206}Pb	^{207}Pb	^{206}Pb	^{207}Pb	^{206}Pb	^{238}U	^{206}Pb	^{235}U	^{207}Pb	^{206}Pb	^{238}U	^{206}Pb		
	mg	ppm	ppm	ppm	pg	mol	pg	pg	pg	pg	pg	pg	pg	pg	pg	pg	pg	pg	pg	pg	pg	pg	
12PSC96																							
A	0.0041	36	0.424	1.6	0.2553	98.60%	21	0.30	1323	0.133	0.050813	2.555	0.289310	2.734	0.041294	0.273	0.682	232.34	58.98	258.02	6.23	260.85	0.70
B	0.0034	69	0.496	3.0	0.4003	98.96%	29	0.35	1779	0.157	0.051257	0.630	0.290703	0.674	0.041134	0.153	0.391	252.40	14.49	259.11	1.54	259.86	0.39
C	0.0041	45	0.494	2.0	0.3166	98.83%	26	0.31	1578	0.157	0.051633	2.038	0.292633	2.170	0.041105	0.257	0.557	269.21	46.73	260.63	4.99	259.68	0.65
D	0.0026	141	0.604	6.5	0.6297	98.85%	27	0.60	1603	0.194	0.052143	0.895	0.296348	0.943	0.041220	0.214	0.335	291.69	20.44	263.54	2.19	260.39	0.54
E	0.0029	25	0.387	1.2	0.1251	96.03%	7	0.42	464	0.121	0.050405	3.208	0.287018	3.354	0.041298	0.317	0.498	213.73	74.29	256.21	7.59	260.88	0.81
F	0.0029	46	0.425	2.0	0.2319	98.66%	22	0.26	1379	0.136	0.052114	1.379	0.296982	1.460	0.041331	0.236	0.415	290.39	31.49	264.04	3.39	261.08	0.60

(a) A, B etc. are labels for fractions composed of single zircon grains or fragments; all fractions annealed and chemically abraded after Mattinson (2005) and Scoates and Friedman (2008).

(b) Nominal fraction weights estimated from photomicrographic grain dimensions, adjusted for partial dissolution during chemical abrasion.

(c) Nominal U and total Pb concentrations subject to uncertainty in photomicrographic estimation of weight and partial dissolution during chemical abrasion.

(d) Model Th/U ratio calculated from radiogenic $^{208}\text{Pb}/^{206}\text{Pb}$ ratio and $^{207}\text{Pb}/^{235}\text{U}$ age.

(e) Pb* and Pb represent radiogenic and common Pb, respectively; mol % $^{206}\text{Pb}^*$ with respect to radiogenic, blank and initial common Pb.

(f) Measured ratio corrected for spike and fractionation only. Mass discrimination of 0.25% \pm 0.03 per amu based on analysis of NBS-982; all Daily analyses.

(g) Corrected for fractionation, spike, and common Pb; up to 0.3 pg of common Pb was assumed to be procedural blank: $^{206}\text{Pb}/^{204}\text{Pb} = 18.50 \pm 1.0\%$; $^{207}\text{Pb}/^{204}\text{Pb} = 15.50 \pm 1.0\%$; $^{208}\text{Pb}/^{206}\text{Pb} = 38.40 \pm 1.0\%$ (all uncertainties 1-sigma). Excess over blank was assigned to initial common Pb with Stacey and Kramers (1975) model Pb composition at 260 Ma.

(h) Errors are 2-sigma, propagated using the algorithms of Schmitz and Schoene (2007) and Crowley et al. (2007).

(i) Calculations are based on the decay constants of Jaffey et al. (1971), $^{206}\text{Pb}/^{238}\text{U}$ and $^{207}\text{Pb}/^{235}\text{U}$ ages corrected for initial disequilibrium in $^{230}\text{Th}/^{238}\text{U}$ using Th/U [magma] = 3.

**Fig. 7.** Red sandstone, Tyughton Formation, sample site 12PSC-91.

measurements, propagates all analytical errors, and calculates isotopic ratios and ages. Corrections for mass and elemental fractionation were made by bracketing analyses of unknown grains with replicate analyses of the Plešovice zircon standard. A typical analytical session consisted of four analyses of the Plešovice standard zircon, followed by two analyses of the Temora2 zircon standard, five analyses of unknown zircons, two standard analyses, then five unknown analyses. Each session was completed with two Temora2 and four Plešovice standard analyses. The Temora2 reference zircon was analyzed as an unknown in order to monitor the reproducibility of the age determinations on a run-to-run basis. Final interpretation and plotting of the analytical results employed the ISOPLOT software of Ludwig (2003).

4.2. Sample 12PSC-91, Tyughton Formation, red sandstone

Sample 12PSC-91 was collected from the basal unit of the Tyughton Formation a few 10s of m southeast of its (unexposed) contact with the Wineglass assemblage (Figs. 3, 4; 527964E, 5736192N, UTM Zone 10 NAD 83). The exposure at this locality is predominantly red and grey-green, fine- to coarse-grained sandstone, intercalated with red siltstone and red pebble conglomerate. The sample is from a red, coarse-grained sandstone bed that includes about 10% secondary calcite as small patches and veins (Fig. 7). It is composed mainly of feldspathic, felsic to mafic volcanic lithic grains, but also includes saussuritic plagioclase, quartz (including some grains with embayed margins), epidote-altered aggregates derived from mafic mineral or lithic grains, siltstone, quartzite, and tonalite. The tonalite grains (equigranular intergrowths of plagioclase and quartz) are uncommon but tend to be larger (2 mm) than the other detrital grains (≤ 1.5 mm).

Sixty-four detrital zircon grains were analyzed from sample 12PSC-91, yielding $^{206}\text{Pb}/^{238}\text{U}$ ages ranging from 271.9 Ma to 212.7 Ma (Table 2). Two strong peaks and an intervening trough on the probability density curve (Fig. 8) permit subdivision into two populations. The older population (n=39) consists mainly

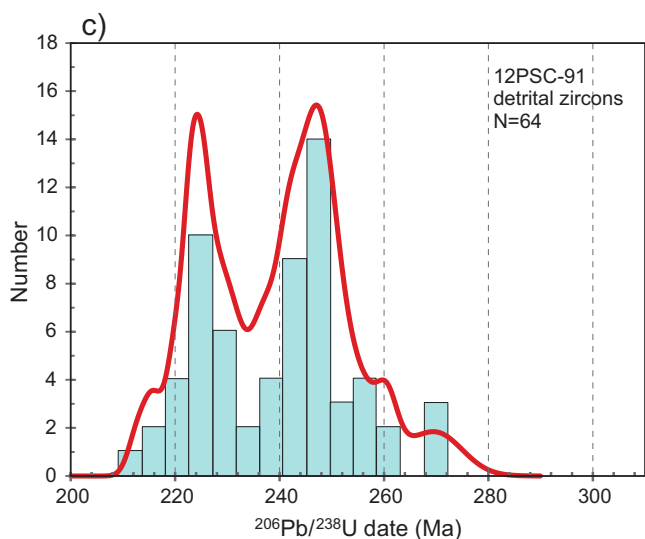
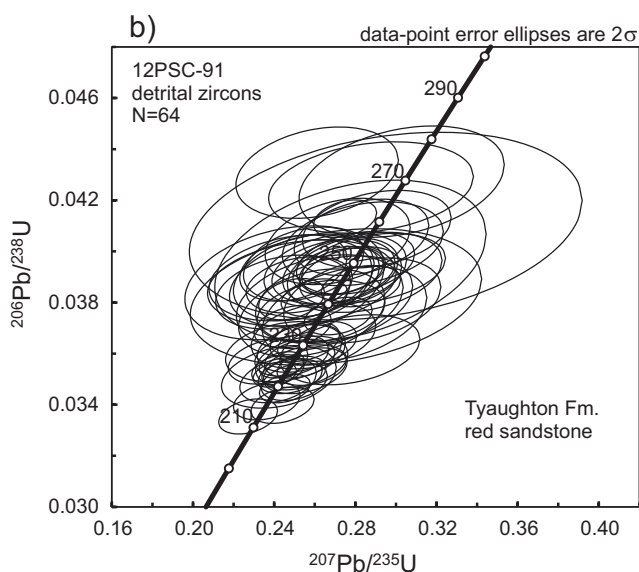
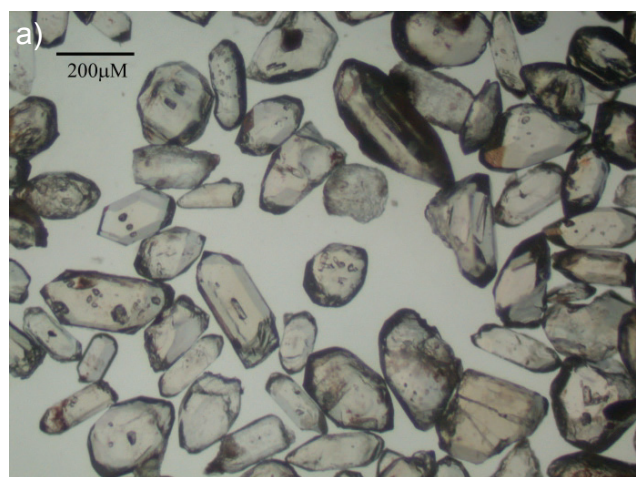


Fig. 8. U-Pb data for detrital zircons from sample 12PSC-91. **a)** Photomicrograph of zircons. **b)** Concordia plot of all grains. **c)** Histogram of detrital zircon ages and superimposed probability density curve.

of Late Permian to Middle Triassic grains (260.7 to 237.1 Ma) with a peak at 247 Ma on the probability density curve, but also includes an outlier of three grains with early Middle Permian ages (271.9, 269.7, 268.3 Ma). The younger population ($n=25$) comprises Late Triassic grains (234.6 to 212.7 Ma) with a peak at 224 Ma on the probability density curve. The youngest grains (212.7, 215.4, 216.4 Ma) suggest a middle to late Norian maximum depositional age.

4.3. Sample 12PSC-97, Tyaughton Formation, green sandstone

Sample 12PSC-97 was collected from the upper part of the Tyaughton Formation, 1300 m northwest of sample 12PSC-91 (Figs. 3, 4; 527054E, 5737072N, UTM Zone 10 NAD 83). It comes from an outcrop of green medium- to coarse-grained sandstone that weathers greenish-brown and shows no discernible bedding (Fig. 9). The sandstone consists mainly of very-fine-grained lithic grains that are variably altered to sericite±epidote. Some of these grains contain microphenocrysts of feldspar and/or quartz and were derived from felsic volcanic rock, but others may have been derived from siltstone. The sandstone also contains grains of sericite±epidote-altered plagioclase, quartz (most markedly angular, some rounded with embayed margins), and mafic mineral or lithic grains altered to epidote and chlorite.

The $^{206}\text{Pb}/^{238}\text{U}$ ages for the analyzed zircons ($n=64$) range from 237.7 to 205.6 Ma, with a peak at 219 Ma on the probability density curve (Table 3; Fig. 10). The oldest grain (237.7 Ma) is near the Middle Triassic/Late Triassic boundary, and the other grains span most of the Late Triassic. The youngest grains (205.6, 205.7, 208.5, 208.7, 208.9 Ma) suggest a late Norian or Rhaetian maximum depositional age.

4.4. Sample 12PSC-98, Hurley Formation, green sandstone

Sample 12PSC-98 was collected from an outcrop on the south side of Highway 20 (527054E, 5737072N, UTM Zone 10, NAD 83), 8 km west-northwest of Riske Creek (Fig. 2). These rocks are part of a package of siliciclastic rocks and limestones that were identified as Hurley Formation (Cadwallader Group) by Rusmore and Woodsworth (1991) and mapped as a folded thrust panel (Bald Mountain slice) by Read (1992, 1993) and Mahoney et al. (2013). Limestone units in this fault panel, of unknown stratigraphic relationship to the siliciclastic rocks sampled along the highway, have yielded late Carnian and early Norian conodonts (Mahoney et al., 2013). The outcrop along Highway 20 comprises green gritty to pebbly sandstone (Fig. 11) intercalated with medium to thick beds of pebble conglomerate. Aphanitic and quartz-feldspar-phyric felsic volcanic clasts predominate, but the conglomerates and pebbly sandstones also contain angular to subrounded clasts of limestone, aphanitic and plagioclase-phyric mafic volcanic rock, red and green chert, cherty argillite, diabase, and tonalite. Sample 12PSC-98, from the central part of the outcrop, is a green coarse-grained sandstone with scattered lithic granules. Detrital grains are mainly felsic volcanic rock (some with



Fig. 9. Massive green sandstone, Tyaughton Formation, sample site 12PSC-97.

quartz and/or feldspar phenocrysts) but also include quartz, plagioclase, pyroxene, and chlorite-epidote-altered mafic volcanic rock.

Sixty-two detrital zircon grains were analyzed from sample 12PSC-98, yielding late Middle Triassic and Late Triassic $^{206}\text{Pb}/^{238}\text{U}$ ages ranging from 239.8 Ma to 210 Ma (Table 4). The probability density curve shows a strong peak at 223 Ma, and subsidiary peaks at 219 Ma, 230 Ma and 239 Ma (Fig. 12). The youngest grains (210, 210.6, 212.5, 212.5, 213.6 Ma) suggest a late Norian maximum depositional age.

5. Discussion

Read (1993) mapped Mesozoic siliciclastic rocks that rest unconformably above Late Permian rocks of the Wineglass assemblage as a single unit, which he considered Early Jurassic because it included an exposure of siltstone with Toarcian fossils (Hickson, 1990). Schiarizza (2013), on lithologic grounds, assigned the lower part of this Mesozoic succession to the Tyaughton Formation (Late Triassic), and the upper part, including the fossiliferous siltstones, to the Ladner Group (Early to Middle Jurassic). Detrital zircons from samples 12PSC-91 and 12PSC-97 (Figs. 3 and 4) corroborate the interpretation of Schiarizza (2013) by providing maximum depositional ages consistent with the late Norian to Rhaetian age of the Tyaughton Formation in its type area (Tozer, 1979; Umhoefer, 1990; Umhoefer and Tipper, 1998). The very strong similarity between the detrital zircon populations of samples 12PSC-97 (Tyaughton Formation) and 12PSC-98 (Hurley Formation in a different fault panel) also corroborate the interpretation that both samples are from Triassic rocks of the same terrane, and support the long-held view that the Late Triassic siliciclastic rocks of Cadwallader terrane (Hurley and Tyaughton formations) were sourced from an associated Late Triassic magmatic arc (Rusmore, 1987; Rusmore et al., 1988; Umhoefer, 1990).

Sample 12PSC-91 (lower part of the Tyaughton formation near its contact with underlying Wineglass assemblage) yielded,

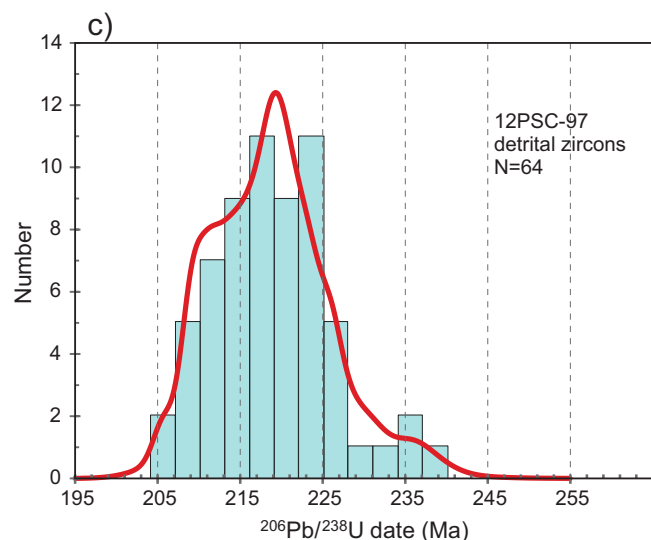
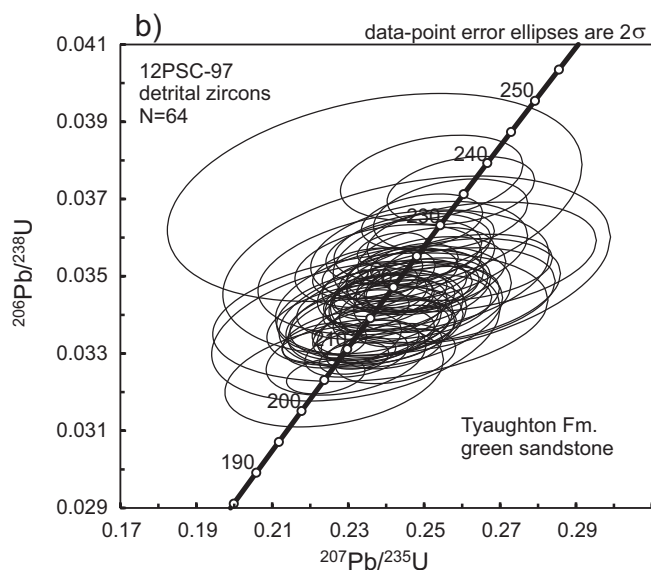
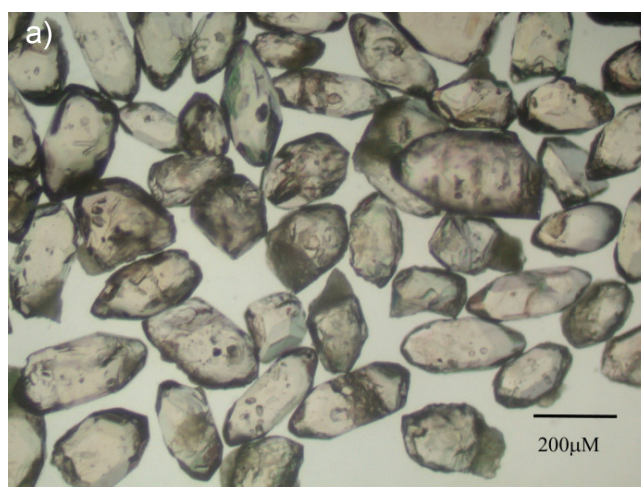


Fig. 10. U-Pb data for detrital zircons from sample 12PSC-97. **a)** Photomicrograph of zircons. **b)** Concordia plot of all grains. **c)** Histogram of detrital zircon ages and superimposed probability density curve.

Table 2. Zircon U-Pb laser ablation analytical data for sample 12PSC-91, Tyaughton Formation red sandstone.

Sample no. Analysis ID	Isotopic Ratios					Isotopic Ages							
	²⁰⁷ Pb/ ²³⁵ U	1σ	²⁰⁶ Pb/ ²³⁸ U	1σ	ρ	²⁰⁷ Pb/ ²⁰⁶ Pb	1σ	²⁰⁷ Pb/ ²³⁵ U	1σ	²⁰⁶ Pb/ ²³⁸ U	1σ	²⁰⁷ Pb/ ²⁰⁶ Pb	1σ
	(abs)	(abs)	(abs)	(abs)		(abs)	(abs)	(Ma)	(Ma)	(Ma)	(Ma)	(Ma)	(Ma)
12PSC91-1	0.2586	0.0148	0.0376	0.0007	0.33	0.0546	0.0028	233.5	11.9	237.9	4.37	395.4	109
12PSC91-2	0.2837	0.0162	0.0403	0.0007	0.29	0.0520	0.0027	253.6	12.8	254.7	4.13	283.7	113
12PSC91-3	0.3028	0.0207	0.0427	0.0009	0.31	0.0515	0.0030	268.6	16.1	269.7	5.51	261.5	130
12PSC91-4	0.2594	0.0125	0.0367	0.0005	0.30	0.0533	0.0023	234.2	10.1	232.4	3.27	339.7	96.1
12PSC91-5	0.2950	0.0396	0.0410	0.0015	0.27	0.0490	0.0059	262.5	31	259	9.26	149.2	260
12PSC91-6	0.2776	0.0273	0.0396	0.0013	0.33	0.0617	0.0054	248.8	21.7	250.6	7.98	664.9	178
12PSC91-7	0.2420	0.0077	0.0350	0.0004	0.32	0.0504	0.0014	220	6.31	221.5	2.24	212.2	64.1
12PSC91-8	0.2721	0.0093	0.0392	0.0004	0.29	0.0501	0.0015	244.4	7.45	248.1	2.44	200.4	69.3
12PSC91-9	0.2830	0.0136	0.0406	0.0006	0.31	0.0525	0.0022	253.1	10.7	256.3	3.76	308.8	92.7
12PSC91-10	0.2716	0.0068	0.0375	0.0003	0.32	0.0541	0.0012	244	5.45	237.1	1.88	376.9	48.6
12PSC91-11	0.2423	0.0116	0.0351	0.0005	0.30	0.0521	0.0023	220.3	9.45	222.3	3.13	290.8	95.9
12PSC91-12	0.2546	0.0142	0.0390	0.0007	0.32	0.0497	0.0024	230.3	11.5	246.6	4.3	179.2	110
12PSC91-13	0.2545	0.0121	0.0395	0.0006	0.31	0.0511	0.0022	230.2	9.8	249.8	3.65	244	95
12PSC91-14	0.2727	0.0116	0.0392	0.0005	0.32	0.0527	0.0020	244.8	9.27	248.1	3.31	315.8	82.9
12PSC91-15	0.2696	0.0158	0.0381	0.0007	0.31	0.0524	0.0027	242.4	12.7	241.1	4.35	302.6	114
12PSC91-16	0.2479	0.0064	0.0351	0.0003	0.31	0.0510	0.0012	224.9	5.24	222.5	1.77	242.6	52.4
12PSC91-17	0.2702	0.0144	0.0393	0.0006	0.28	0.0527	0.0026	242.8	11.5	248.3	3.64	317	106
12PSC91-18	0.2890	0.0145	0.0394	0.0006	0.28	0.0516	0.0023	257.8	11.4	248.9	3.42	267.2	100
12PSC91-19	0.2437	0.0046	0.0356	0.0002	0.32	0.0496	0.0008	221.4	3.71	225.3	1.29	176.9	38.3
12PSC91-20	0.2442	0.0064	0.0340	0.0003	0.33	0.0518	0.0012	221.8	5.19	215.4	1.78	274.5	52.2
12PSC91-21	0.2612	0.0080	0.0364	0.0004	0.32	0.0551	0.0015	235.7	6.41	230.5	2.2	415.1	59
12PSC91-22	0.2847	0.0156	0.0392	0.0006	0.30	0.0543	0.0027	254.3	12.3	247.7	3.95	382.5	106
12PSC91-23	0.2500	0.0172	0.0390	0.0007	0.26	0.0464	0.0029	226.5	14	246.4	4.27	18.4	145
12PSC91-24	0.2451	0.0201	0.0388	0.0009	0.29	0.0538	0.0041	222.6	16.4	245.2	5.63	363.9	162
12PSC91-25	0.2419	0.0053	0.0354	0.0002	0.31	0.0497	0.0010	219.9	4.31	224.1	1.5	181.5	44.7
12PSC91-26	0.2524	0.0107	0.0387	0.0005	0.27	0.0481	0.0019	228.6	8.66	244.7	2.8	104.2	88.5
12PSC91-27	0.2444	0.0136	0.0384	0.0006	0.28	0.0484	0.0025	222	11.1	243	3.64	118	117
12PSC91-28	0.2598	0.0067	0.0382	0.0003	0.31	0.0502	0.0012	234.5	5.39	241.6	1.84	204.9	52.3
12PSC91-29	0.2502	0.0063	0.0352	0.0003	0.30	0.0507	0.0011	226.7	5.11	223.3	1.69	226.4	51.1
12PSC91-30	0.2834	0.0158	0.0381	0.0007	0.32	0.0536	0.0026	253.4	12.5	240.9	4.22	353.9	106
12PSC91-31	0.2456	0.0121	0.0361	0.0005	0.27	0.0504	0.0023	223	9.85	228.5	3.01	212	102
12PSC91-32	0.2487	0.0074	0.0359	0.0003	0.31	0.0514	0.0014	225.5	6.04	227.5	2.06	257.7	60.6
12PSC91-33	0.2801	0.0119	0.0396	0.0005	0.30	0.0541	0.0021	250.8	9.43	250.1	3.11	375.9	82.9
12PSC91-34	0.2713	0.0146	0.0404	0.0007	0.32	0.0508	0.0024	243.7	11.7	255.2	4.29	232.1	104
12PSC91-35	0.2550	0.0086	0.0354	0.0004	0.33	0.0546	0.0017	230.7	6.96	224.2	2.42	394	65.6
12PSC91-36	0.2747	0.0166	0.0376	0.0008	0.34	0.0556	0.0029	246.4	13.2	237.7	4.69	435.3	113
12PSC91-37	0.2705	0.0293	0.0382	0.0011	0.26	0.0504	0.0050	243.1	23.4	241.8	6.75	213.3	215
12PSC91-38	0.2532	0.0144	0.0388	0.0007	0.31	0.0507	0.0026	229.2	11.7	245.2	4.27	227.7	112
12PSC91-39	0.2750	0.0063	0.0413	0.0003	0.32	0.0512	0.0010	246.7	5.05	260.7	1.84	250.5	45.9
12PSC91-40	0.2827	0.0080	0.0386	0.0003	0.30	0.0520	0.0013	252.8	6.32	244.4	2.08	286.2	55.9
12PSC91-41	0.2906	0.0150	0.0409	0.0006	0.29	0.0539	0.0025	259	11.8	258.2	3.83	368.4	101
12PSC91-42	0.2612	0.0164	0.0431	0.0007	0.27	0.0469	0.0027	235.6	13.2	271.9	4.49	45	131
12PSC91-43	0.2878	0.0206	0.0425	0.0007	0.24	0.0502	0.0033	256.8	16.3	268.3	4.53	204	147
12PSC91-44	0.2495	0.0108	0.0394	0.0005	0.31	0.0507	0.0020	226.2	8.78	248.8	3.28	225.4	86.8
12PSC91-45	0.2486	0.0066	0.0381	0.0003	0.32	0.0501	0.0012	225.5	5.4	241.2	2.03	197.3	53.6
12PSC91-46	0.2551	0.0070	0.0365	0.0003	0.32	0.0523	0.0013	230.7	5.67	231	1.99	298.9	54.5
12PSC91-47	0.2693	0.0124	0.0392	0.0005	0.29	0.0509	0.0021	242.1	9.92	247.9	3.21	238.2	93.6
12PSC91-48	0.2625	0.0168	0.0380	0.0008	0.31	0.0495	0.0028	236.7	13.5	240.6	4.63	170.5	126
12PSC91-49	0.2585	0.0070	0.0355	0.0003	0.31	0.0526	0.0013	233.5	5.62	224.8	1.84	312.6	53.8
12PSC91-50	0.2453	0.0051	0.0346	0.0002	0.32	0.0517	0.0010	222.7	4.17	219.5	1.44	270.2	42
12PSC91-52	0.2631	0.0129	0.0377	0.0005	0.27	0.0513	0.0023	237.2	10.3	238.2	3.14	252.4	99.4
12PSC91-53	0.2773	0.0141	0.0362	0.0006	0.30	0.0560	0.0026	248.5	11.2	228.9	3.49	453.6	99.2
12PSC91-54	0.2364	0.0067	0.0341	0.0003	0.31	0.0515	0.0013	215.4	5.5	216.4	1.85	262.3	57.8
12PSC91-55	0.2272	0.0059	0.0335	0.0003	0.32	0.0509	0.0012	207.9	4.9	212.7	1.74	236.6	53.1
12PSC91-56	0.2492	0.0078	0.0371	0.0003	0.29	0.0491	0.0014	225.9	6.33	234.6	2.11	151	64.8
12PSC91-57	0.2526	0.0071	0.0358	0.0003	0.31	0.0493	0.0012	228.7	5.74	226.8	1.92	164	56.9
12PSC91-58	0.2526	0.0086	0.0362	0.0004	0.31	0.0513	0.0015	228.7	6.93	229.2	2.38	251.9	67.6
12PSC91-59	0.2370	0.0080	0.0357	0.0004	0.30	0.0493	0.0015	216	6.58	226.1	2.26	164	69.7
12PSC91-60	0.2500	0.0067	0.0349	0.0003	0.32	0.0531	0.0013	226.5	5.41	221.1	1.85	334.6	53.1
12PSC91-61	0.2537	0.0190	0.0388	0.0007	0.24	0.0453	0.0032	229.6	15.4	245.2	4.28	0.1	124
12PSC91-62	0.2777	0.0103	0.0390	0.0005	0.33	0.0549	0.0018	248.8	8.16	246.8	2.94	407.1	70.7
12PSC91-63	0.2536	0.0093	0.0357	0.0004	0.31	0.0536	0.0018	229.5	7.52	226	2.56	354.8	71.9
12PSC91-64	0.2403	0.0044	0.0352	0.0002	0.31	0.0503	0.0008	218.7	3.57	222.9	1.27	208.8	36.7
12PSC91-65	0.2732	0.0084	0.0392	0.0004	0.31	0.0522	0.0014	245.2	6.73	248	2.3	293.6	61.3

Table 3. Zircon U-Pb laser ablation analytical data for sample 12PSC-97, Tyaughton Formation green sandstone.

Sample no. Analysis ID	Isotopic Ratios						Isotopic Ages						
	$^{207}\text{Pb}/^{235}\text{U}$	1σ (abs)	$^{206}\text{Pb}/^{238}\text{U}$	1σ (abs)	ρ	$^{207}\text{Pb}/^{206}\text{Pb}$	1σ (abs)	$^{207}\text{Pb}/^{235}\text{U}$	1σ (Ma)	$^{206}\text{Pb}/^{238}\text{U}$	1σ (Ma)	$^{207}\text{Pb}/^{206}\text{Pb}$	1σ (Ma)
12PSC97-1	0.2372	0.0094	0.0337	0.0004	0.31	0.0492	0.0018	216.1	7.73	213.7	2.6	158.8	81.5
12PSC97-2	0.2241	0.0042	0.0324	0.0002	0.31	0.0486	0.0008	205.3	3.51	205.6	1.2	126	39.5
12PSC97-3	0.2412	0.0120	0.0340	0.0006	0.33	0.0527	0.0023	219.4	9.84	215.5	3.52	314.9	97.4
12PSC97-4	0.2322	0.0056	0.0330	0.0003	0.32	0.0491	0.0011	212	4.58	209.3	1.57	150.3	49.2
12PSC97-5	0.2607	0.0142	0.0355	0.0006	0.30	0.0540	0.0027	235.2	11.4	224.8	3.59	369	106
12PSC97-6	0.2363	0.0081	0.0342	0.0003	0.29	0.0505	0.0016	215.3	6.64	216.8	2.13	216.1	70.8
12PSC97-7	0.2400	0.0057	0.0339	0.0003	0.31	0.0505	0.0011	218.4	4.66	214.8	1.57	216.8	48.5
12PSC97-8	0.2507	0.0078	0.0344	0.0004	0.33	0.0528	0.0015	227.1	6.36	218	2.18	319.9	61.8
12PSC97-9	0.2478	0.0082	0.0342	0.0003	0.30	0.0500	0.0015	224.8	6.67	216.8	2.1	195.4	68.1
12PSC97-10	0.2465	0.0078	0.0349	0.0003	0.30	0.0504	0.0015	223.8	6.39	221.1	2.06	212.2	65.7
12PSC97-12	0.2447	0.0084	0.0356	0.0004	0.29	0.0493	0.0015	222.2	6.83	225.6	2.21	161.4	70.9
12PSC97-13	0.2385	0.0050	0.0345	0.0002	0.32	0.0508	0.0010	217.2	4.11	218.8	1.41	231.4	43
12PSC97-14	0.2385	0.0180	0.0339	0.0007	0.26	0.0537	0.0039	217.2	14.8	215.2	4.24	358	154
12PSC97-15	0.2474	0.0047	0.0353	0.0002	0.33	0.0526	0.0009	224.5	3.84	223.7	1.36	312.3	37.9
12PSC97-16	0.2410	0.0070	0.0343	0.0003	0.31	0.0515	0.0013	219.2	5.71	217.6	1.92	261.4	58.5
12PSC97-17	0.2406	0.0101	0.0353	0.0004	0.30	0.0507	0.0020	218.9	8.23	223.4	2.72	225.3	86.4
12PSC97-18	0.2381	0.0060	0.0344	0.0003	0.31	0.0502	0.0011	216.9	4.88	217.9	1.68	203.7	50.9
12PSC97-19	0.2358	0.0052	0.0347	0.0003	0.33	0.0505	0.0010	215	4.26	220.1	1.54	217.1	44.7
12PSC97-20	0.2597	0.0079	0.0372	0.0004	0.32	0.0519	0.0014	234.4	6.4	235.6	2.22	280.6	60.7
12PSC97-21	0.2442	0.0060	0.0351	0.0003	0.31	0.0505	0.0011	221.9	4.88	222.3	1.65	218.7	49.8
12PSC97-22	0.2334	0.0037	0.0330	0.0002	0.32	0.0507	0.0007	213	3.07	209.3	1.06	225.1	32.4
12PSC97-23	0.2438	0.0050	0.0346	0.0002	0.32	0.0524	0.0010	221.5	4.1	219.2	1.45	304.5	41.1
12PSC97-24	0.2295	0.0086	0.0329	0.0004	0.32	0.0503	0.0017	209.8	7.11	208.7	2.51	207	75.6
12PSC97-25	0.2347	0.0046	0.0341	0.0002	0.33	0.0511	0.0009	214.1	3.81	216.2	1.36	246	40
12PSC97-26	0.2367	0.0066	0.0335	0.0003	0.31	0.0508	0.0013	215.7	5.38	212.3	1.78	230.8	56.7
12PSC97-27	0.2263	0.0118	0.0324	0.0005	0.32	0.0480	0.0022	207.2	9.73	205.7	3.37	98	107
12PSC97-28	0.2316	0.0037	0.0329	0.0002	0.32	0.0511	0.0007	211.5	3.09	208.5	1.09	245.5	32.7
12PSC97-29	0.2487	0.0117	0.0356	0.0005	0.32	0.0495	0.0021	225.5	9.49	225.7	3.3	173.2	93.7
12PSC97-30	0.2356	0.0090	0.0338	0.0004	0.31	0.0512	0.0018	214.8	7.38	214.2	2.48	249.6	77.2
12PSC97-31	0.2446	0.0157	0.0351	0.0007	0.29	0.0500	0.0029	222.2	12.8	222.4	4.13	194.4	129
12PSC97-32	0.2321	0.0155	0.0336	0.0007	0.33	0.0516	0.0031	211.9	12.8	212.9	4.6	265.5	131
12PSC97-33	0.2358	0.0101	0.0341	0.0005	0.31	0.0481	0.0018	214.9	8.25	216.1	2.82	102.7	87.2
12PSC97-34	0.2284	0.0064	0.0334	0.0003	0.32	0.0488	0.0012	208.9	5.3	211.6	1.88	137.1	57.5
12PSC97-35a	0.2487	0.0057	0.0347	0.0003	0.31	0.0508	0.0010	225.5	4.64	219.8	1.57	230.1	46.3
12PSC97-36	0.2493	0.0062	0.0347	0.0003	0.31	0.0505	0.0011	226	5.02	220	1.66	216.9	50
12PSC97-37	0.2419	0.0127	0.0344	0.0006	0.32	0.0499	0.0023	220	10.4	217.9	3.63	188.1	104
12PSC97-38	0.2395	0.0078	0.0337	0.0003	0.28	0.0498	0.0015	218	6.35	213.4	1.95	184.7	67.2
12PSC97-39a	0.2399	0.0074	0.0336	0.0003	0.33	0.0520	0.0014	218.4	6.06	212.8	2.13	284.8	61
12PSC97-40	0.2455	0.0065	0.0348	0.0003	0.31	0.0505	0.0012	222.9	5.27	220.3	1.76	218.2	53.4
12PSC97-41	0.2447	0.0093	0.0347	0.0004	0.32	0.0494	0.0017	222.3	7.61	219.6	2.63	164.8	76.6
12PSC97-42	0.2316	0.0094	0.0338	0.0004	0.31	0.0494	0.0018	211.5	7.75	214	2.68	166.5	82.5
12PSC97-43	0.2425	0.0065	0.0329	0.0003	0.33	0.0523	0.0012	220.4	5.3	208.9	1.78	298.2	52.9
12PSC97-44	0.2380	0.0095	0.0339	0.0004	0.31	0.0506	0.0018	216.7	7.8	214.8	2.59	223.6	81
12PSC97-45	0.2548	0.0122	0.0345	0.0005	0.31	0.0516	0.0022	230.4	9.85	218.6	3.19	265.3	94.7
12PSC97-46	0.2570	0.0083	0.0366	0.0004	0.32	0.0530	0.0015	232.3	6.7	231.7	2.39	330.5	63
12PSC97-47	0.2520	0.0098	0.0376	0.0005	0.31	0.0490	0.0017	228.2	7.97	237.7	2.8	149.1	78.9
12PSC97-48	0.2506	0.0074	0.0355	0.0003	0.31	0.0526	0.0014	227	6	224.8	1.97	312.6	59
12PSC97-49	0.2494	0.0071	0.0347	0.0003	0.30	0.0522	0.0013	226.1	5.77	220.2	1.88	294.4	57
12PSC97-50	0.2358	0.0053	0.0333	0.0002	0.31	0.0510	0.0010	215	4.32	211.2	1.46	239.4	45
12PSC97-51	0.2518	0.0069	0.0359	0.0003	0.32	0.0506	0.0012	228	5.56	227.6	1.91	221.1	54.5
12PSC97-52	0.2370	0.0223	0.0370	0.0011	0.32	0.0511	0.0043	215.9	18.3	234.4	6.86	244.8	183
12PSC97-53	0.2415	0.0055	0.0332	0.0002	0.32	0.0520	0.0010	219.6	4.47	210.5	1.48	284.8	45.3
12PSC97-54	0.2556	0.0124	0.0346	0.0006	0.33	0.0515	0.0022	231.1	10	219.5	3.44	263.8	93.8
12PSC97-55	0.2480	0.0209	0.0353	0.0010	0.32	0.0508	0.0038	225	17	223.4	5.91	232.3	163
12PSC97-56	0.2613	0.0092	0.0352	0.0004	0.28	0.0518	0.0015	235.7	7.39	223.2	2.19	274.7	66.6
12PSC97-57	0.2495	0.0065	0.0364	0.0003	0.30	0.0498	0.0012	226.1	5.31	230.6	1.81	184	52.9
12PSC97-58	0.2380	0.0061	0.0351	0.0003	0.30	0.0497	0.0011	216.8	4.99	222.2	1.7	181.8	52.2
12PSC97-59	0.2352	0.0059	0.0351	0.0003	0.31	0.0482	0.0011	214.4	4.87	222.2	1.71	111.2	51.8
12PSC97-60	0.2505	0.0086	0.0351	0.0004	0.32	0.0522	0.0016	227	6.98	222.2	2.46	294.8	67.4
12PSC97-61	0.2391	0.0054	0.0345	0.0002	0.31	0.0505	0.0010	217.7	4.43	218.4	1.5	219.3	45.8
12PSC97-62	0.2416	0.0038	0.0357	0.0002	0.32	0.0511	0.0007	219.8	3.08	226.1	1.13	243.9	30.7
12PSC97-63	0.2469	0.0084	0.0357	0.0004	0.30	0.0504	0.0015	224.1	6.86	226.4	2.26	211.3	69.6
12PSC97-64	0.2237	0.0046	0.0333	0.0002	0.31	0.0493	0.0009	205	3.79	211.1	1.34	163.3	41.8
12PSC97-65	0.2444	0.0050	0.0337	0.0002	0.32	0.0520	0.0009	222.1	4.08	213.7	1.39	285.5	40.3

Table 4. Zircon U-Pb laser ablation analytical data for sample 12PSC-98, Hurley Formation sandstone.

Sample no. Analysis ID	Isotopic Ratios					Isotopic Ages							
	$^{207}\text{Pb}/^{235}\text{U}$	1σ	$^{206}\text{Pb}/^{238}\text{U}$	1σ	ρ	$^{207}\text{Pb}/^{206}\text{Pb}$	1σ	$^{207}\text{Pb}/^{235}\text{U}$	1σ	$^{206}\text{Pb}/^{238}\text{U}$	1σ	$^{207}\text{Pb}/^{206}\text{Pb}$	1σ
	(abs)	(abs)	(abs)	(abs)		(abs)	(abs)	(Ma)	(Ma)	(Ma)	(Ma)	(Ma)	(Ma)
12PSC98-2	0.2523	0.0079	0.0376	0.0004	0.31	0.0495	0.0014	228.5	6.4	237.9	2.28	173.2	64.1
12PSC98-3	0.2470	0.0145	0.0350	0.0006	0.30	0.0502	0.0027	224.1	11.8	221.9	3.89	204.6	119
12PSC98-4	0.2601	0.0086	0.0354	0.0004	0.34	0.0536	0.0016	234.7	6.89	224.2	2.43	355.4	64.2
12PSC98-5	0.2463	0.0061	0.0352	0.0003	0.30	0.0508	0.0012	223.6	4.99	222.8	1.63	231.6	51.6
12PSC98-6	0.2389	0.0048	0.0344	0.0002	0.30	0.0499	0.0009	217.5	3.94	218	1.34	191.1	41.9
12PSC98-7	0.2512	0.0062	0.0353	0.0003	0.32	0.0521	0.0012	227.5	5.05	223.4	1.75	287.7	50.2
12PSC98-8	0.2292	0.0070	0.0332	0.0003	0.30	0.0503	0.0014	209.5	5.75	210.6	1.88	206.5	63.7
12PSC98-9	0.2485	0.0087	0.0343	0.0004	0.32	0.0516	0.0016	225.4	7.08	217.6	2.45	266.6	70
12PSC98-10	0.2451	0.0060	0.0344	0.0003	0.31	0.0502	0.0011	222.6	4.87	218.2	1.59	204.4	50.7
12PSC98-11	0.2503	0.0097	0.0354	0.0004	0.32	0.0519	0.0018	226.8	7.85	224.1	2.73	279.2	77.4
12PSC98-12	0.2409	0.0057	0.0349	0.0003	0.31	0.0503	0.0011	219.2	4.62	221.2	1.58	207.3	48.7
12PSC98-13	0.2427	0.0058	0.0341	0.0003	0.31	0.0502	0.0011	220.6	4.73	215.9	1.57	202.5	49.2
12PSC98-14	0.2383	0.0056	0.0335	0.0002	0.29	0.0482	0.0010	217	4.57	212.5	1.45	111.2	49.4
12PSC98-15	0.2428	0.0057	0.0339	0.0002	0.30	0.0498	0.0011	220.7	4.62	215	1.51	185.1	48.5
12PSC98-16	0.2423	0.0076	0.0338	0.0003	0.30	0.0482	0.0014	220.3	6.24	214.4	1.99	110	66
12PSC98-17	0.2333	0.0084	0.0331	0.0004	0.32	0.0513	0.0017	212.9	6.89	210	2.35	255	73.5
12PSC98-18	0.2474	0.0049	0.0345	0.0002	0.32	0.0499	0.0009	224.5	4.01	218.4	1.34	191.9	41.1
12PSC98-19	0.2514	0.0063	0.0346	0.0003	0.31	0.0526	0.0012	227.7	5.07	218.9	1.66	312.7	50.4
12PSC98-20	0.2341	0.0071	0.0335	0.0003	0.29	0.0494	0.0014	213.6	5.82	212.5	1.82	168.4	63.7
12PSC98-21	0.2478	0.0061	0.0341	0.0003	0.32	0.0492	0.0011	224.8	4.94	216	1.68	157	50.1
12PSC98-22	0.2526	0.0078	0.0349	0.0004	0.33	0.0522	0.0014	228.7	6.32	220.9	2.17	295.3	61.6
12PSC98-23	0.2466	0.0116	0.0347	0.0005	0.33	0.0521	0.0022	223.8	9.42	219.8	3.36	289.4	92.8
12PSC98-24	0.2501	0.0060	0.0343	0.0003	0.30	0.0503	0.0011	226.6	4.89	217.1	1.57	207.7	49.8
12PSC98-25	0.2495	0.0043	0.0345	0.0002	0.32	0.0514	0.0008	226.1	3.52	218.3	1.2	257.8	35.4
12PSC98-26	0.2472	0.0048	0.0354	0.0002	0.32	0.0516	0.0009	224.3	3.87	224.2	1.4	269.7	38.9
12PSC98-27	0.2573	0.0116	0.0350	0.0005	0.32	0.0534	0.0022	232.5	9.36	222	3.15	343.8	88.4
12PSC98-28	0.2396	0.0062	0.0357	0.0003	0.30	0.0496	0.0012	218.1	5.09	226	1.75	178	54.1
12PSC98-29	0.2478	0.0164	0.0362	0.0008	0.32	0.0504	0.0030	224.8	13.3	229.3	4.79	213.6	130
12PSC98-30	0.2380	0.0042	0.0350	0.0002	0.32	0.0503	0.0008	216.8	3.48	221.7	1.25	207.3	36.7
12PSC98-31	0.2610	0.0118	0.0367	0.0005	0.31	0.0520	0.0021	235.4	9.51	232.2	3.23	287	90.1
12PSC98-32	0.2606	0.0123	0.0371	0.0006	0.33	0.0526	0.0022	235.2	9.89	234.7	3.57	311.7	92.3
12PSC98-33	0.2446	0.0060	0.0363	0.0003	0.32	0.0512	0.0011	222.1	4.88	229.6	1.76	247.8	50
12PSC98-34	0.2502	0.0056	0.0366	0.0003	0.31	0.0502	0.0010	226.7	4.55	231.6	1.57	202.2	46.2
12PSC98-35	0.2444	0.0067	0.0364	0.0003	0.30	0.0486	0.0012	222	5.44	230.5	1.89	127	56.9
12PSC98-36	0.2478	0.0074	0.0379	0.0003	0.30	0.0491	0.0013	224.8	6.01	239.8	2.13	153	61.8
12PSC98-37	0.2623	0.0223	0.0377	0.0010	0.32	0.0551	0.0042	236.5	17.9	238.7	6.37	416.3	162
12PSC98-38	0.2567	0.0080	0.0379	0.0004	0.30	0.0485	0.0014	232	6.49	239.7	2.18	123.4	65.5
12PSC98-39	0.2578	0.0064	0.0354	0.0003	0.31	0.0506	0.0011	232.9	5.15	224.4	1.7	224.4	50.4
12PSC98-40	0.2535	0.0059	0.0354	0.0003	0.33	0.0518	0.0011	229.4	4.77	224.3	1.66	274.7	46.9
12PSC98-41	0.2477	0.0060	0.0371	0.0003	0.30	0.0493	0.0011	224.7	4.85	234.8	1.69	160	50
12PSC98-42	0.2591	0.0067	0.0378	0.0003	0.32	0.0518	0.0012	233.9	5.41	239.5	1.91	276.3	52.3
12PSC98-43	0.2572	0.0058	0.0364	0.0003	0.33	0.0515	0.0010	232.4	4.72	230.4	1.68	262.4	45.5
12PSC98-44	0.2616	0.0060	0.0363	0.0003	0.32	0.0535	0.0011	235.9	4.84	230	1.68	348.4	45.8
12PSC98-45	0.2350	0.0071	0.0357	0.0004	0.32	0.0515	0.0014	214.3	5.86	225.9	2.19	263.4	61.5
12PSC98-46	0.2434	0.0085	0.0349	0.0004	0.29	0.0506	0.0016	221.2	6.96	221.3	2.22	222.9	72.8
12PSC98-47	0.2577	0.0055	0.0364	0.0003	0.32	0.0508	0.0010	232.8	4.45	230.4	1.55	230.8	43.2
12PSC98-48	0.2384	0.0098	0.0350	0.0004	0.29	0.0510	0.0019	217.1	8	221.6	2.6	240	84.5
12PSC98-49	0.2498	0.0047	0.0346	0.0002	0.32	0.0516	0.0009	226.4	3.85	219.5	1.33	267.1	38.3
12PSC98-50	0.2507	0.0077	0.0352	0.0003	0.31	0.0515	0.0014	227.1	6.24	223.1	2.11	263.9	62.2
12PSC98-51	0.2382	0.0055	0.0352	0.0003	0.32	0.0497	0.0010	217	4.53	223	1.61	180.3	47.9
12PSC98-52	0.2597	0.0084	0.0356	0.0004	0.33	0.0521	0.0015	234.4	6.73	225.7	2.37	291.7	63.2
12PSC98-53	0.2356	0.0185	0.0369	0.0009	0.32	0.0489	0.0035	214.8	15.2	233.6	5.75	144.7	157
12PSC98-54	0.2640	0.0070	0.0356	0.0003	0.33	0.0536	0.0013	237.9	5.6	225.7	1.91	353.4	52.3
12PSC98-55	0.2508	0.0055	0.0359	0.0003	0.32	0.0506	0.0010	227.2	4.46	227.3	1.55	223.2	44.5
12PSC98-58	0.2438	0.0051	0.0364	0.0002	0.32	0.0507	0.0009	221.5	4.13	230.3	1.51	225.8	42.3
12PSC98-59	0.2435	0.0064	0.0352	0.0003	0.34	0.0532	0.0013	221.3	5.22	222.9	1.91	336.7	52.6
12PSC98-60	0.2517	0.0066	0.0363	0.0003	0.33	0.0524	0.0012	228	5.35	229.6	1.91	304.5	52.3
12PSC98-61	0.2404	0.0164	0.0370	0.0008	0.32	0.0486	0.0030	218.7	13.4	234.2	4.98	126.1	138
12PSC98-62	0.2334	0.0116	0.0337	0.0005	0.32	0.0503	0.0023	213	9.55	213.6	3.35	209.3	100
12PSC98-63	0.2471	0.0044	0.0368	0.0002	0.34	0.0502	0.0008	224.2	3.57	233	1.34	203.3	36
12PSC98-64	0.2521	0.0069	0.0367	0.0003	0.32	0.0525	0.0013	228.3	5.55	232	2.02	308.4	54.2
12PSC98-65	0.2453	0.0108	0.0348	0.0005	0.31	0.0516	0.0021	222.8	8.84	220.6	3.01	266.9	88.7



Fig. 11. Pebbly sandstone, Hurley Formation, near sample site 12PSC-98.

in addition to Late Triassic detrital zircons, a predominant population of Late Permian to Middle Triassic zircons not seen in the younger sample from the Tyaughton Formation (12PSC-97) or in the sample from the Hurley Formation (12PSC-98). This population of zircons is inferred to have been derived from the Wineglass assemblage and/or related rocks that form the older component of Cadwallader terrane in this region. The oldest zircons in this population are the same age as the dated volcanic and plutonic rocks of the Wineglass assemblage, and it is suspected that the Lower and Middle Triassic grains are from younger, eroded and/or covered components of the assemblage. A Late Permian to Middle Triassic age range thus inferred for the Wineglass assemblage is consistent with its correlation with the Sitlika volcanic unit and the Kutcho assemblage (Schiarizza, 2013), because each of these units contains volcanic and intrusive rocks with an age range from Late Permian to Middle Triassic (Fig. 15 of Schiarizza, 2013).

5.1. Tyaughton Creek facies of Cadwallader terrane

Cadwallader terrane in south-central British Columbia comprises Late Permian to Middle Jurassic rocks that are exposed in numerous small and large outcrop belts that have been dispersed by major dextral strike-slip faults of the Yalakom and Fraser systems, and are commonly separated from one another by large areas of younger rock (Fig. 13). The terrane was originally defined for exposures near Gold Bridge (Fig. 13; Rusmore et al., 1988) where it includes two distinct stratigraphic successions, referred to as the Camelsfoot facies and the Tyaughton Creek facies (Schiarizza et al., 1997). Both of these facies also occur in the other major outcrop belts of Cadwallader terrane, near Tatlayoko and Chilko lakes, and along the lower reaches of the Chilcotin River (Fig. 13). Their original paleogeographic relationship is unknown, although the Camelsfoot facies most commonly occurs west of the Tyaughton Creek facies. The Camelsfoot facies consists of the Cadwallader Group, including Middle to Late Triassic basalt of

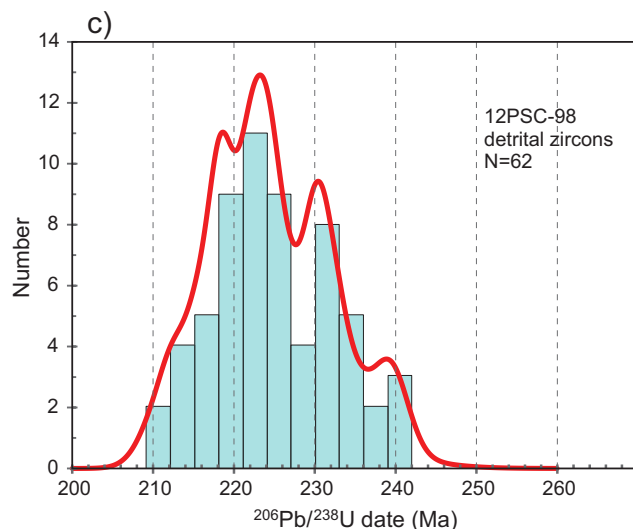
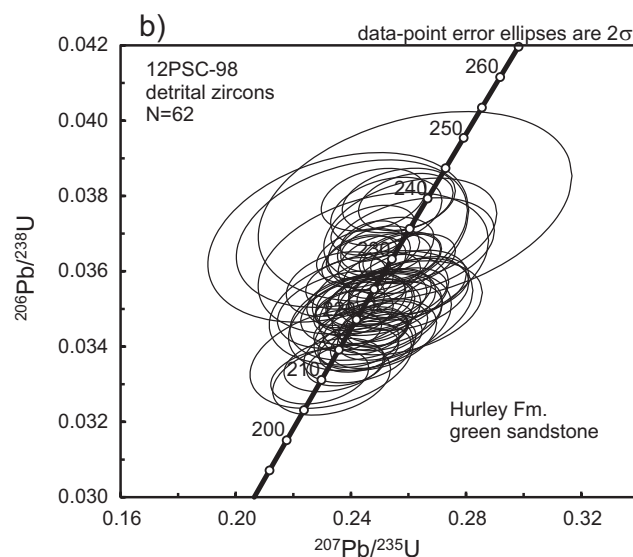
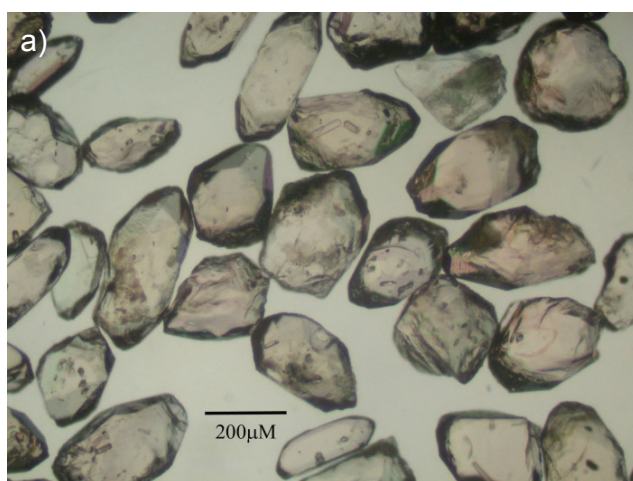


Fig. 12. U-Pb data for detrital zircons from sample 12PSC-98. **a)** Photomicrograph of zircons. **b)** Concordia plot of all grains. **c)** Histogram of detrital zircon ages and superimposed probability density curve.

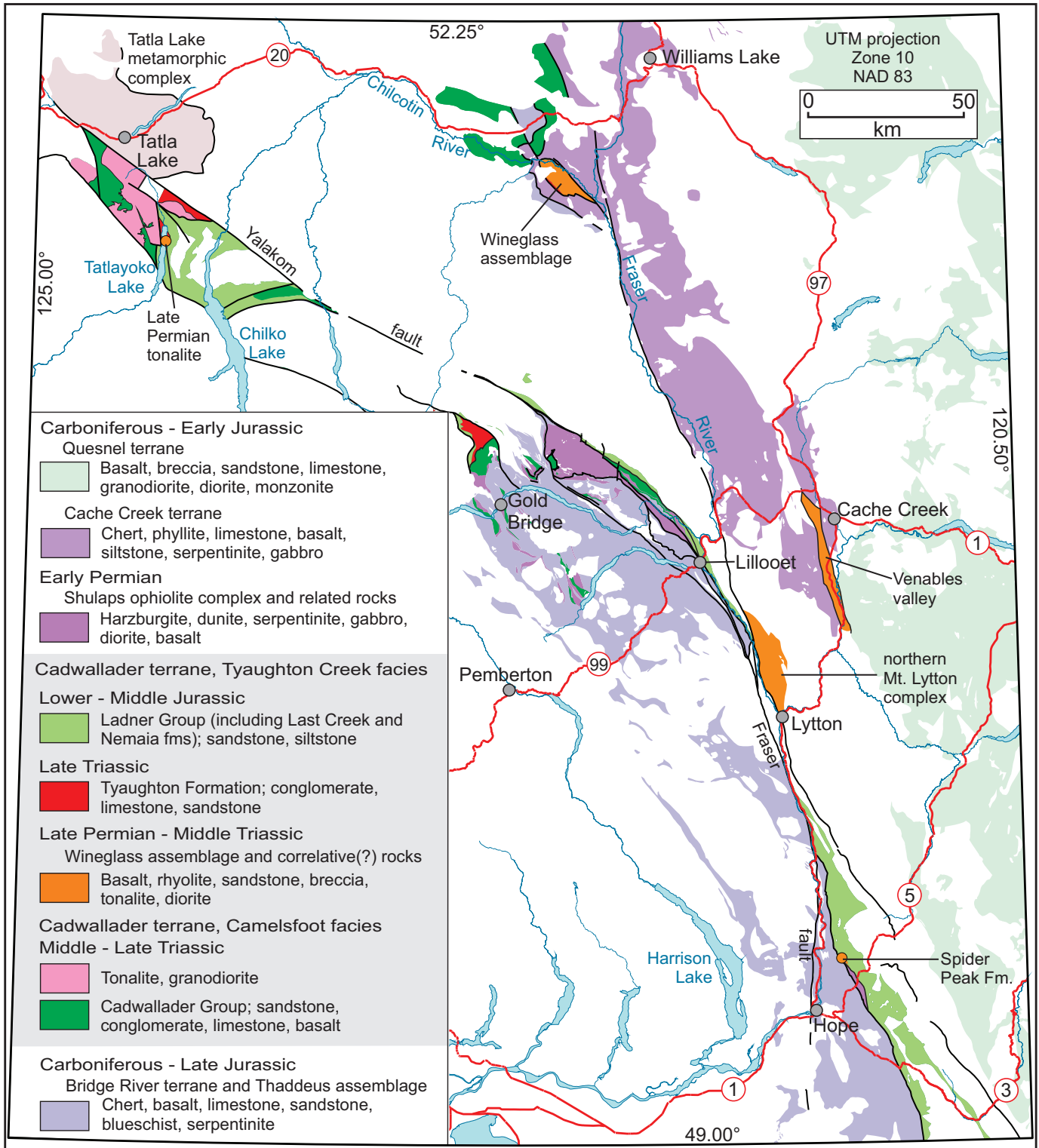


Fig. 13. Map of south-central British Columbia highlighting Cadwallader terrane and adjacent Paleozoic to mid-Mesozoic terranes. Geology from Cui et al. (2017). Uncoloured areas are mainly younger rocks, including Late Jurassic to Cretaceous siliciclastic rocks of the Tyaughton-Methow basin and Late Jurassic to Eocene granitoid intrusions.

the Pioneer Formation and overlying Late Triassic (Carnian to Norian) sandstone, conglomerate and limestone of the Hurley Formation (Rusmore, 1987). The Tyaughton Creek facies, which includes rocks in the Chilcotin River window, has three components separated by unconformities or disconformities: Late Permian (and younger?) volcanic and intrusive rocks; latest Triassic sedimentary rocks of the Tyaughton Formation; and Early to Middle Jurassic sedimentary rocks (Ladner Group and correlatives).

The lower part of the Tyaughton Creek facies is represented by basalt, rhyolite and tonalite of the Wineglass assemblage (Late Permian), which underlies the Tyaughton Formation in the Chilcotin River window (Schiarizza, 2013; this study), and also by Late Permian tonalite that underlies the Tyaughton Formation on the east shore of Tatlayoko Lake (Fig. 13; Schiarizza et al., 1995, 2002). It may also be represented by the northern part of the Mount Lytton complex (Fig. 13), which includes Late Permian or Early Triassic tonalite that Friedman and van der Heyden (1992) correlate with the Wineglass pluton, and by basalt of the Spider Peak Formation, which underlies the Ladner Group (upper part of the Tyaughton Creek facies) in a small area north-northeast of Hope (Fig. 13; Ray, 1990).

The middle part of the Tyaughton Creek facies comprises sedimentary rocks of the Tyaughton Formation (Late Triassic). The most complete section of the formation is in its type area, north-northwest of Gold Bridge (Fig. 13), where it includes a lower unit of red conglomerates and sandstones, ('Lower red beds' of Umhoefer, 1990) a middle unit of massive and bedded limestones ('Massive limestone' and 'Monotis limestone' of Umhoefer, 1990), and an upper unit of green sandstones, pebble conglomerates and calcarenites ('Lower green clastics', 'Cassianella beds', and 'Upper green clastics' of Umhoefer, 1990). Conglomerates in the lower unit contain clasts of felsic to mafic volcanic rock, limestone, and granitoid plutonic rock. The middle and upper units, dated with macrofossils, are late Norian and Rhaetian (Tozer, 1979; Umhoefer, 1990; Umhoefer and Tipper, 1998). The base of the Tyaughton Formation does not occur in its type area, but the formation also occurs 120 km to the northwest (Umhoefer and Tipper, 1998), where exposures at the north end of Tatlayoko Lake rest nonconformably above Late Permian tonalite (Fig. 13; Schiarizza et al., 1995, 2002). Likewise, the Tyaughton Formation in the Chilcotin River window, correlated with the lower and upper units of the type area (limestone unit missing), rests unconformably above Permian volcanic rocks of the Wineglass assemblage.

The upper part of the Tyaughton Creek facies comprises Lower to Middle Jurassic sedimentary rocks, mainly grey siltstones and sandstones, with local pebble conglomerates. North of Gold Bridge they are represented by upper Hettangian to Middle Bajocian rocks of the Last Creek Formation, which overlie the Tyaughton Formation disconformably (Umhoefer, 1990; Umhoefer and Tipper, 1998). Correlative rocks to the northwest, near Tatlayoko and Chilko lakes (Fig. 13), are assigned to the Nemaia Formation (Sinemurian to Bajocian; Umhoefer and Tipper, 1998; Schiarizza et al., 2002), which

apparently overlies the Tyaughton Formation near the north end of Tatlayoko Lake, although the contact is not exposed. The Nemaia Formation can be traced southeastward, with significant dextral offsets along the Yalakom and Fraser faults, into identical rocks of the Lower to Middle Jurassic Ladner Group, which forms a linear belt extending from near Lytton to the international boundary (Fig. 13; Mahoney, 1993; Schiarizza et al., 1997). The base of the Ladner Group is exposed locally northeast of Hope where it rests unconformably above basalts of the Spider Peak Formation (Ray, 1990), which may belong in the lower part of the Tyaughton Creek facies. The middle part, the Tyaughton Formation, is apparently missing, although it may be present as polymictic conglomerates, up to 70 m thick, that occur at the Spider Peak-Ladner contact (Ray, 1990).

5.2. Cadwallader terrane correlatives in central and northern British Columbia

Schiarizza (2013) correlated the Wineglass assemblage with the volcanic unit of the Sitlika assemblage in central British Columbia and the Kutcho assemblage in northern British Columbia (Fig. 14). These units have traditionally been included in Cache Creek terrane, although Mihalynuk et al. (2017) suggest they should be treated as a separate terrane. Schiarizza (2013) included the Wineglass assemblage in Cadwallader terrane, implying that the correlative rocks in central and northern British Columbia are also part of Cadwallader terrane. Here, we support this terrane assignment by pointing out that the rocks that overlie both the volcanic unit of the Sitlika assemblage and the Kutcho assemblage are very similar to the middle and upper parts of the Tyaughton Creek facies (Tyaughton Formation and Ladner Group) in southern British Columbia.

In central British Columbia the Wineglass-correlative Sitlika volcanic unit is unconformably(?) overlain by siliciclastic rocks and limestones of the Sitlika clastic unit, which is best exposed in a continuous belt, almost 100 km long, east of the volcanic unit (Figs. 14, 15; Schiarizza, 2000; Schiarizza et al., 2000). The clastic unit, as described by Schiarizza and Payie (1997) and Schiarizza et al. (1998), consists of sandstone, slate, and siltstone, with less common conglomerate, limestone, and calcarenite. Conglomerate commonly forms the base of the unit, and has a clast composition (mainly felsic volcanic plus limestone, mafic volcanic rock, and granitic rock) very similar to conglomerates in the lower part of the Tyaughton Formation. Limestones are mainly in the lower part of the unit, directly above the basal conglomerate where it is present, and therefore have a stratigraphic position similar to the main limestone occurrences in the Tyaughton Formation. The only biochronologic constraint for the unit comes from conodonts extracted from a calcarenite bed in the central part of the main belt of exposures, which are assigned a late Norian to Rhaetian age (M.J. Orchard in Struik et al., 2007, sample 97-PSC-19-2), showing that it is, at least in part, the same age as the Tyaughton Formation. In addition, a small population of detrital zircons (n=6) analyzed from a sample of sandstone collected from the

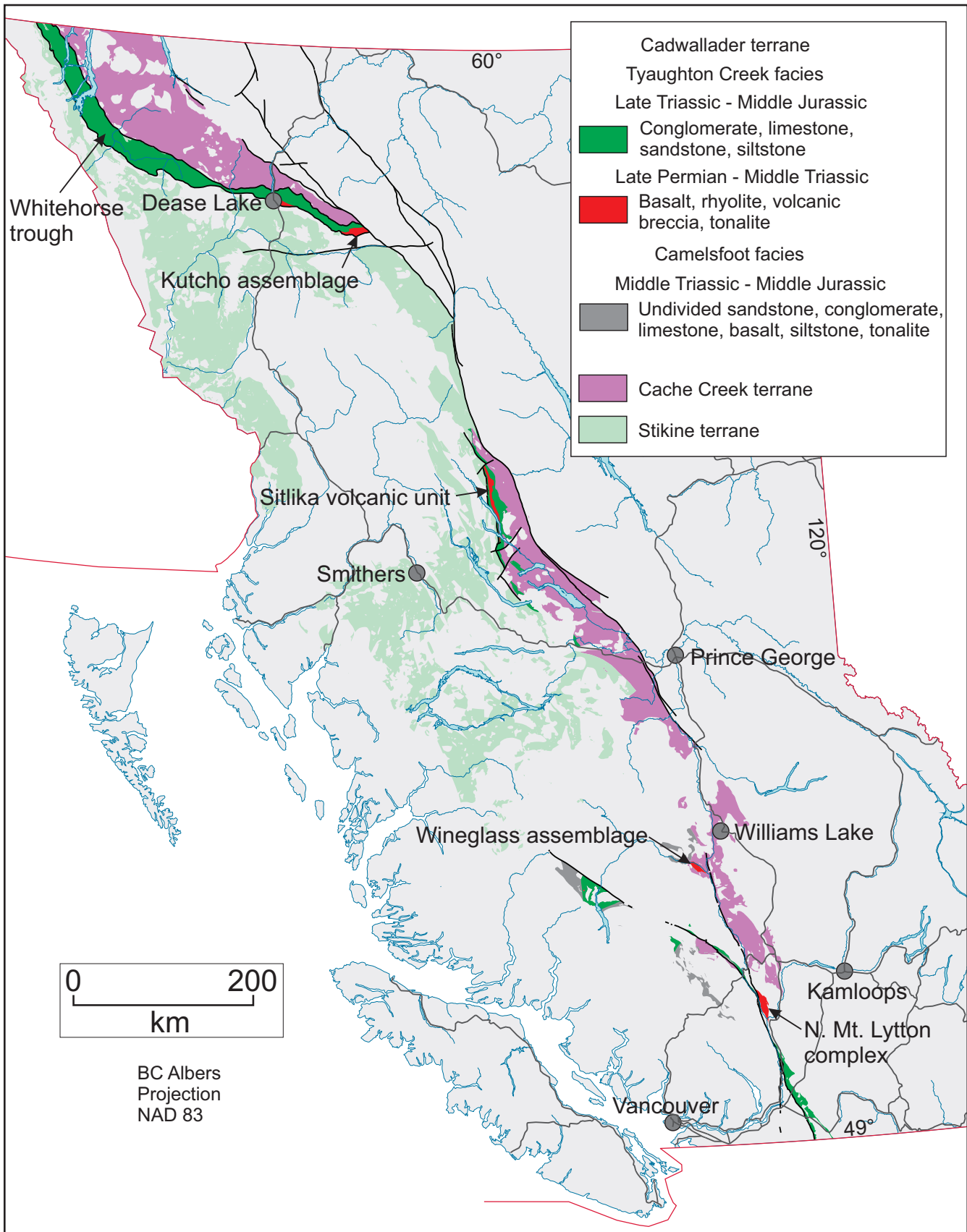


Fig. 14. Map highlighting Permian-Jurassic rocks comprising the Tyauhton Creek facies of Cadwallader terrane in southern British Columbia and correlative rocks in central and northern British Columbia. Geology from Cui et al. (2017).

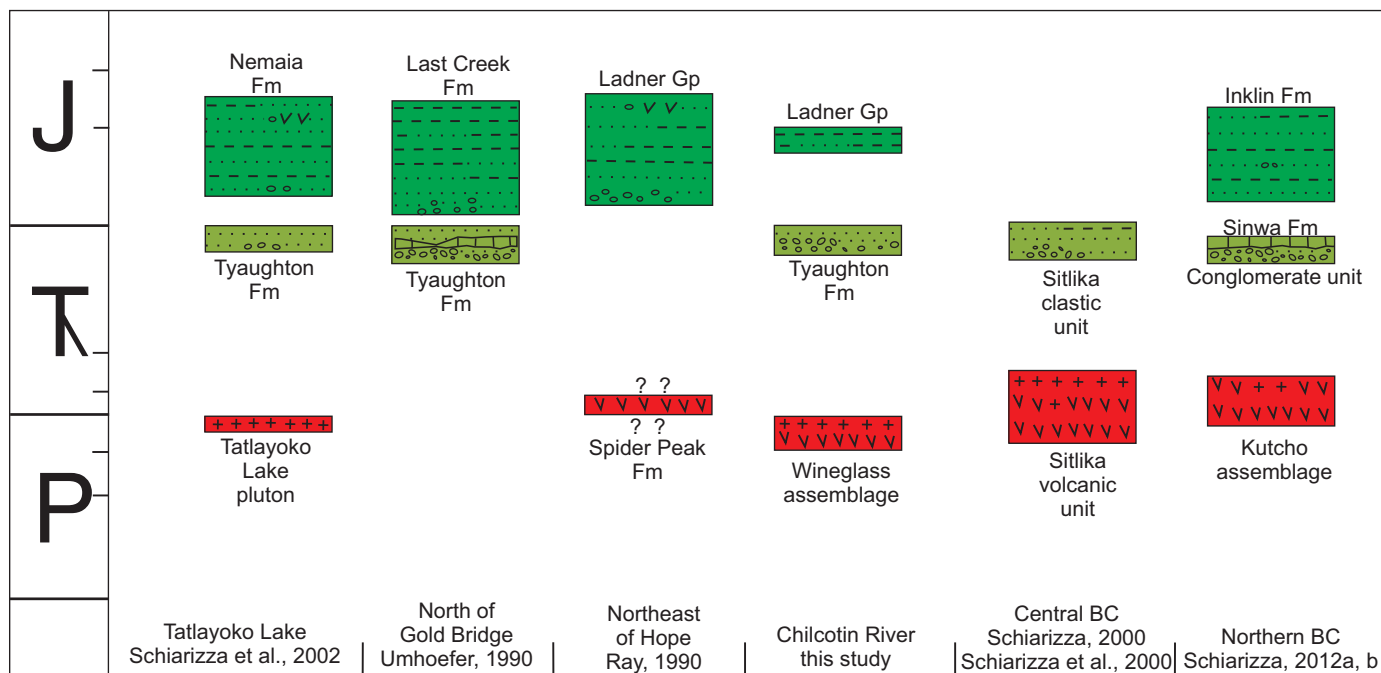


Fig. 15. Schematic stratigraphic sections for the Tyaughton Creek facies of Cadwallader terrane in southern British Columbia, and correlative rocks in central and northern British Columbia.

northern part of the main exposure belt contained only Late Triassic grains ranging from 226 to 201.7 Ma (M. Villeneuve, in Struik et al., 2007, sample 97-PSC-22). Despite the very small sample size this is very similar to the age range of detrital zircons from the upper part of the Tyaughton Formation in the Chilcotin River window (Fig. 10).

In northern British Columbia, the Kutcho assemblage is in a narrow belt of mainly Lower to Middle Jurassic siliciclastic rocks (Whitehorse trough, represented by the Inklin Formation) that forms the boundary between the main exposures of Cache Creek terrane to the northeast and Stikine terrane to the southwest (Fig. 14). The Kutcho assemblage is best exposed at the east end of the belt, adjacent to Kutcho Creek where it and overlying rocks were mapped by Schiarizza (2012a, b). Here, the Kutcho assemblage is unconformably overlain by upper Triassic rocks herein correlated with the Tyaughton Formation, which are in turn unconformably or disconformably overlain by Lower Jurassic siliciclastic rocks of the Inklin Formation, herein correlated with the Ladner Group (Fig. 15). The upper Triassic rocks include a lower conglomerate unit (with clasts of felsic volcanic rock, mafic volcanic rock, limestone and tonalite) and overlying massive to well-bedded limestone (Sinwa Formation) which together are very similar to the lower and middle parts of the Tyaughton Formation in its type area. The Sinwa limestone is not dated at Kutcho Creek, but exposures 180 km west-northwest of Dease Lake, near the type area of the formation, contain the ammonoid *Halorites* cf., *H. americanus* Hyatt and Smith and the bivalve *Monotis subcircularis* Gabb (E.T. Tozer in Souther, 1971), both of which characterize the Late Norian fauna of the *Monotis* limestone member of the Tyaughton Formation (Umhoefer and

Tipper, 1978). The Inklin Formation in the Kutcho Creek area comprises metasandstone, metasiltstone, and slate, with local intercalations of pebble conglomerate and rare narrow lenses of limestone (Schiarizza, 2012a). It typically overlies the Sinwa Formation but in places, where the Sinwa and conglomerate unit are missing, it is directly above the Kutcho assemblage. No fossils have been extracted from the formation in this area, but detrital zircons from the base of the formation at one locality indicate an Early Jurassic maximum depositional age (Schiarizza, 2012b), and rocks included in, or correlated with, the formation to the northwest contain Early and early Middle Jurassic fossils (Mihalynuk, 1999; Colpron, 2011). The Inklin Formation is correlated with the Ladner Group on the basis of lithology, inferred Early to Middle Jurassic age, and unconformable or disconformable relationship with underlying rocks correlated with the Tyaughton Formation.

The Inklin Formation forms a continuous narrow belt, deformed by southwest-verging folds and thrust faults, that extends from Kutcho Creek to the northern border of British Columbia (Fig. 14; Christie, 1957; Aitken, 1959; Souther, 1971; Gabrielse, 1988; Mihalynuk, 1999), and from there into southern Yukon where it is mapped as the Richthofen Formation of the Laberge Group (Colpron, 2011). The Richthofen Formation, like the Inklin Formation and Ladner Group, is predominantly lithic sandstone, siltstone and mudstone, and it contains fossils ranging from early Sinemurian to Aalenian (Colpron, 2011), very similar to the fossil ages from the Ladner Group and correlatives in southern British Columbia (Tipper and Umhoefer, 1998). The Richthofen Formation, in southern Yukon, is underlain by the Aksala Formation (Late Triassic), which comprises three members (Colpron, 2011): Mandanna

member, mainly maroon to red weathering sandstone and polymictic conglomerate; Hancock member, mainly massive to thick bedded limestone, dated at many localities as late Norian; and Casca member, mudstone, siltstone and calcareous sandstone, with interbedded bioclastic limestone and igneous or limestone-clast conglomerate. This stratigraphy is remarkably similar to that of the Tyaughton Formation in its type area (Umhoefer, 1990; Umhoefer and Tipper, 1998); a similarity that is even more pronounced when the overlying Jurassic rocks are also compared. The Aksala Formation is part of the Lewes River Group, a Triassic arc-derived succession in Yukon that is typically considered part of Stikine terrane (Colpron, 2011). The correlations proposed here (Aksala with Tyaughton, Richthofen with Ladner) suggest that the Lewes River Group might, at least in part, be part of Cadwallader terrane.

6. Summary

Along the Chilcotin River, 50 km southwest of Williams Lake, late Paleozoic and Mesozoic rocks of Cadwallader terrane are exposed in a structural window beneath overthrust Cache Creek terrane. These Cadwallader terrane rocks include Late Permian volcanic and plutonic rocks of the Wineglass assemblage, unconformably overlying sandstones and conglomerates correlated with the Tyaughton Formation (latest Triassic) and Early to Middle Jurassic siltstones and sandstones assigned to the Ladner Group. Rhyolite from the top of the Wineglass assemblage, dated by U-Pb zircon chemical abrasion thermal ionization mass spectrometry (CA-TIMS), crystallized at 260.8 ± 0.3 Ma, confirming a Late Permian age reported by Read (1993). Detrital zircons from red sandstone in the lower part of the Tyaughton Formation, dated by Laser Ablation Inductively Coupled Plasma Mass Spectrometry (LA-ICP-MS), include a population of mainly Late Permian to Middle Triassic grains (260.7 to 237.1 Ma), probably derived from the underlying Wineglass assemblage, and a population of Late Triassic grains (234.6 to 212.7 Ma) inferred to have been derived from Late Triassic volcanic and plutonic rocks exposed elsewhere in Cadwallader terrane. Detrital zircons were also analyzed from a sample of green sandstone in the upper part of the Tyaughton Formation, yielding only Late Triassic grains (237.7 to 205.6 Ma). The youngest zircons from the two samples indicate middle to late Norian and late Norian to Rhaetian maximum depositional ages, respectively, corroborating their correlation with the lower and upper parts of the Tyaughton Formation in its type area.

The Hurley Formation (Late Triassic, Carnian to Norian), a common component of Cadwallader terrane in southern British Columbia, occurs in two fault panels northwest of the Chilcotin River window. Detrital zircons from a Hurley sandstone sample, collected from the Bald Mountain fault panel, comprise latest Middle Triassic to Late Triassic grains (239.8 to 210 Ma) with a range very similar to that of the upper Tyaughton sample (green sandstone), and to the Late Triassic population of the lower Tyaughton sample (red sandstone). These similarities support the interpretation that the Hurley Formation and the

Tyaughton Formation are different parts of the same terrane. The predominance of Late Triassic grains also supports the long-held view that the Late Triassic siliciclastic rocks of Cadwallader terrane (Hurley and Tyaughton formations) were sourced from an associated Late Triassic magmatic arc (Rusmore et al., 1988).

The rocks exposed in the Chilcotin River window are part of a Late Permian to Middle Jurassic succession (Tyaughton Creek facies) that forms a significant part of Cadwallader terrane, but differs from other parts (Camelsfoot facies) comprised mainly of the Cadwallader Group, including Middle to Late Triassic basalts of the Pioneer Formation, and overlying Late Triassic sandstones, conglomerates, and limestones of the Hurley Formation. The Permian to Jurassic rocks of the Tyaughton Creek facies correlate with rocks in central British Columbia (Sitlika assemblage) and northern British Columbia (Kutcho assemblage, Sinwa Formation, Inklin Formation).

Acknowledgments

Robin Chu assisted with fieldwork and the collection of samples for U-Pb dating. Lawrence Aspler (British Columbia Geological Survey) and Jeffery Chiarenzelli (St. Lawrence University) reviewed the paper and offered suggestions that improved it.

References cited

- Aitken, J.D., 1959. Atlin map-area, British Columbia. Geological Survey of Canada, Memoir 307, 89 p.
- Christie, R.L., 1957. Bennett, Cassiar District, British Columbia. Geological Survey of Canada, Map 19-1957; scale 1:253,440.
- Colpron, M., 2011. Geological compilation of Whitehorse trough-Whitehorse (105D), Lake Laberge (105E), and part of Carmacks (115I), Glenlyon (105L), Aishihik Lake (115H), Quiet Lake (105F), and Teslin (105C). Yukon Geological Survey, Geoscience Map 2011-1; scale 1:250,000.
- Cordey, F., and Read, P.B., 1992. Permian and Triassic radiolarian ages from the Cache Creek Complex, Dog Creek and Alkali Lake areas, southwestern British Columbia. In: Current Research, Part E, Geological Survey of Canada Paper 92-1E, pp. 41-51.
- Crowley, J.L., Schoene, B., and Bowring, S.A., 2007. U-Pb dating of zircon in the Bishop Tuff at the millennial scale. *Geology*, 35, 1123-1126.
- Cui, Y., Miller, D., Schiarizza, P., and Diakow, L.J., 2017. British Columbia digital geology. British Columbia Ministry of Energy, Mines and Petroleum Resources, British Columbia Geological Survey Open File 2017-8, 9 p.
- Friedman, R.M., and van der Heyden, P., 1992. Late Permian U-Pb dates for the Farwell and northern Mt. Lytton plutonic bodies, Intermontane Belt, British Columbia. In: Current Research, Part A, Geological Survey of Canada Paper 92-1A, pp. 137-144.
- Gabrielse, H., 1998. Geology of Cry Lake and Dease Lake map areas, north-central British Columbia. Geological Survey of Canada, Bulletin 504, 147 p.
- Gerstenberger, H., and Haase, G., 1997. A highly effective emitter substance for mass spectrometric Pb isotopic ratio determinations. *Chemical Geology*, 136, 309-312.
- Griffin, W.L., Powell, W.J., Pearson, N.J., and O'Reilly, S.Y., 2008. Glitter: Data reduction software for laser ablation ICP-MS. In: Sylvester, P.J., (Ed.), *Laser Ablation ICP-MS in the Earth Sciences: Current Practices and Outstanding Issues*, Mineralogical Association of Canada, Short Course 40, pp. 308-311.

- Hickson, C.J., 1990. A new Frontier Geoscience Project: Chilcotin-Nechako region, central British Columbia. In: Current Research, Part F, Geological Survey of Canada Paper 90-1F, pp. 115-120.
- Jaffey, A.H., Flynn, K.F., Glendenin, L.E., Bentley, W.C., and Essling, A.M., 1971. Precision measurement of half-lives and specific activities of ^{235}U and ^{238}U . Physics Review, C4, 1889-1906.
- Ludwig, K.R., 2003. Isoplot 3.09-A geochronological toolkit for Microsoft Excel. Berkley Geochronology Center, The University of California at Berkeley, Special Publication No. 4.
- Mahoney, J.B., 1993. Facies reconstructions in the Lower to Middle Jurassic Ladner Group, southern British Columbia. In: Current Research, Part A, Geological Survey of Canada Paper 93-1A, pp. 173-182.
- Mahoney, J.B., Hickson, C.J., Haggart, J.W., Schiarizza, P., Read, P.B., Enkin, R.J., van der Heyden, P., and Israel, S., 2013. Geology, Taseko Lakes, British Columbia. Geological Survey of Canada, Open File 6150; scale 1:250,000.
- Mattinson, J.M., 2005. Zircon U-Pb chemical abrasion ("CA-TIMS") method: Combined annealing and multi-step partial dissolution analysis for improved precision and accuracy of zircon ages. Chemical Geology, 220, 47-66.
- Mihalynuk, M.G., 1999. Geology and mineral resources of the Tagish Lake area (NTS 104M/8, 9, 10E, 15 and 104N/12W) northwestern British Columbia. British Columbia Ministry of Energy and Mines, British Columbia Geological Survey Bulletin 105, 217 p.
- Mihalynuk, M.G., and Harker, L.L., 2007. Riske Creek Geology (92O/16W). British Columbia Ministry of Energy, Mines and Petroleum Resources, British Columbia Geological Survey Open File 2007-6; scale 1:50,000.
- Mihalynuk, M.G., Zagorevski, A., English, J.M., Orchard, M.J., Bidgood, A.K., Joyce, N., and Friedman, R.M., 2017. Geology of the Sinwa Creek area, northwest BC (104K/14). In: Geological Fieldwork 2016, British Columbia Ministry of Energy and Mines, British Columbia Geological Survey Paper 2017-1, pp. 153-178.
- Mundil, R., Ludwig, K.R., Metcalfe, I., and Renne, P.R., 2004. Age and timing of the Permian Mass Extinctions: U/Pb Dating of Closed-System Zircons. Science, 305, 1760-1763.
- Ray, G.E., 1990. The geology and mineralization of the Coquihalla gold belt and Hozameen fault system, southwestern British Columbia. British Columbia Ministry of Energy, Mines and Petroleum Resources, British Columbia Geological Survey Bulletin 79, 97 p.
- Read, P.B., 1992. Geology of parts of Riske Creek and Alkali Lake areas, British Columbia. In Current Research, Part A, Geological Survey of Canada Paper 92-1A, pp. 105-112.
- Read, P.B., 1993. Geology of northeast Taseko Lakes map area, southwestern British Columbia. In: Current Research, Part A, Geological Survey of Canada Paper 93-1A, pp. 159-166.
- Rusmore, M.E., 1987. Geology of the Cadwallader Group and the Intermontane-Insular superterrane boundary, southwestern British Columbia. Canadian Journal of Earth Sciences, 24, 2279-2291.
- Rusmore, M.E., and Woodsworth, G.J., 1991. Distribution and tectonic significance of Upper Triassic terranes in the eastern Coast Mountains and adjacent Intermontane Belt, British Columbia. Canadian Journal of Earth Sciences, 28, 532-541.
- Rusmore, M.E., Potter, C.J., and Umhoefer, P.J., 1988. Middle Jurassic terrane accretion along the western edge of the Intermontane superterrane, southwestern British Columbia. Geology, 16, 891-894.
- Schiarizza, P., 2000. Bedrock geology, Old Hogem (western part) (93N/11, 12, 13). British Columbia Ministry of Energy and Mines, British Columbia Geological Survey Open File 2000-33; scale 1:100,000.
- Schiarizza, P., 2012a. Geology of the Kutcho assemblage between the Kehlechoa and Tucho rivers, northern British Columbia (NTS 104I/01, 02). In: Geological Fieldwork 2011, British Columbia Ministry of Energy and Mines, British Columbia Geological Survey Paper 2012-1, pp. 75-98.
- Schiarizza, P., 2012b. Bedrock geology of the upper Kutcho Creek area, parts of NTS 104I/01, 02. British Columbia Ministry of Energy and Mines, British Columbia Geological Survey, Open File 2012-08; scale 1:40,000. Also published as Geological Survey of Canada, Open File 7234.
- Schiarizza, P., 2013. The Wineglass assemblage, lower Chilcotin River, south-central British Columbia: Late Permian volcanic and plutonic rocks that correlate with the Kutcho assemblage of northern British Columbia. In: Geological Fieldwork 2012, British Columbia Ministry of Energy, Mines and Natural Gas, British Columbia Geological Survey Paper 2013-1, pp. 53-70.
- Schiarizza, P., and Payie, G., 1997. Geology of the Sitlika assemblage in the Kenny Creek-Mount Olson area (93N/12, 13), central British Columbia. In: Geological Fieldwork 1996, British Columbia Ministry of Employment and Investment, British Columbia Geological Survey Paper 1997-1, pp. 79-100.
- Schiarizza, P., Melville, D.M., Riddell, J., Jennings, B.K., Umhoefer, P.J., and Robinson, M.J., 1995. Geology and mineral occurrences of the Tatlayoko Lake map area (92N/8, 9 and 10). In: Geological Fieldwork 1994, British Columbia Ministry of Energy, Mines and Petroleum Resources, British Columbia Geological Survey Paper 1995-1, pp. 297-320.
- Schiarizza, P., Gaba, R.G., Glover, J.K., Garver, J.I., and Umhoefer, P.J., 1997. Geology and mineral occurrences of the Taseko-Bridge River area. British Columbia Ministry of Employment and Investment, British Columbia Geological Survey Bulletin 100, 291 p.
- Schiarizza, P., Massey, N., and MacIntyre, D., 1998. Geology of the Sitlika assemblage in the Takla Lake area (93N/3, 4, 5, 6, 12), central British Columbia. In: Geological Fieldwork 1997, British Columbia Ministry of Employment and Investment, British Columbia Geological Survey Paper 1998-1, pp. 4-1 - 4-19.
- Schiarizza, P., Massey, N., and MacIntyre, D.M., 2000. Bedrock geology, Tsayta Lake (93N/3, 4, 5, 6). British Columbia Ministry of Energy and Mines, British Columbia Geological Survey Open File 2000-19; scale 1:100,000.
- Schiarizza, P., Riddell, J., Gaba, R.G., Melville, D.M., Umhoefer, P.J., Robinson, M.J., Jennings, B.K., and Hick, D., 2002. Geology of the Beece Creek-Niut Mountain area, British Columbia (NTS 92N/8, 9, 10; 92O/5, 6, 12). British Columbia Ministry of Energy and Mines, British Columbia Geological Survey Geoscience Map 2002-3; scale 1:100,000.
- Schmitz, M.D., and Schoene, B., 2007. Derivation of isotope ratios, errors, and error correlations for U-Pb geochronology using ^{205}Pb - ^{235}U -(^{233}U)-spiked isotope dilution thermal ionization mass spectrometric data. Geochemistry, Geophysics, Geosystems, 8, Q08006, doi:10.1029/2006GC001492.
- Schoene, B.A., Crowley, J.L., Condon, D.J., Schmitz, M.D., and Bowring, S.A., 2006. Reassessing the uranium decay constants for geochronology using ID-TIMS U-Pb data. Geochimica et Cosmochimica Acta, 70, 426-445.
- Scoates, J.S., and Friedman, R.M., 2008. Precise age of the platinumiferous Merensky Reef, Bushveld Complex, South Africa, by the U-Pb zircon chemical abrasion ID-TIMS technique. Economic Geology, 103, 465-471.
- Sláma, J., Košler, J., Condon, D.J., Crowley, J.L., Gerdes, A., Hanchar, J.M., Horstwood, M.S.A., Morris, G.A., Nasdala, L., Norberg, N., Schaltegger, U., Xchoene, B., Tubrett, M.N., and Whitehouse, M.J., 2007. Plešovice zircon-A new natural reference material for U-Pb and Hf isotopic microanalysis. Chemical Geology, 249, 1-35.
- Souther, J.G., 1971. Geology and mineral deposits of Tulsequah map-area, British Columbia. Geological Survey of Canada, Memoir 362, 84 p.

- Stacey, J.S., and Kramers, J.D., 1975. Approximation of terrestrial lead isotopic evolution by a two-stage model. *Earth and Planetary Science Letters*, 26, 207-221.
- Struik, L.C., MacIntyre, D.G., and Williams, S.P., 2007. Nechako NATMAP project: a digital suite of geoscience information for central British Columbia (NTS map sheets 093N, 093K, 093F, 093G/W, 093L/9, 16, and 093M/1, 2, 7, 8). British Columbia Ministry of Energy, Mines and Petroleum Resources, British Columbia Geological Survey Open File 2007-10. Also published as Geological Survey of Canada, Open File 5623.
- Tafti, R., Mortensen, J.K., Lang, J.R., Rebagliati, M., and Oliver, J.L., 2009. Jurassic U-Pb and Re-Os ages for newly discovered Xietongmen Cu-Au porphyry district, Tibet: Implications for metallogenic epochs in the southern Gangdese Belt. *Economic Geology*, 104, 127-136.
- Thirlwall, M.F., 2000. Inter-laboratory and other errors in Pb isotope analyses investigated using a ^{207}Pb - ^{204}Pb double spike. *Chemical Geology*, 163, 299-322.
- Tipper, H.W., 1978. Taseko Lakes (92O) map area. Geological Survey of Canada Open File 534; scale 1:125,000.
- Tozer, E.T., (1979). Latest Triassic ammonoid faunas and biochronology, western Canada. In: *Current Research, Part B*, Geological Survey of Canada Paper 79-1B, pp. 127-135.
- Umhoefer, P.J., 1990. Stratigraphy and tectonic setting of the upper part of the Cadwallader terrane, southwestern British Columbia. *Canadian Journal of Earth Sciences*, 27, 702-711.
- Umhoefer, P.J., and Tipper, H.W., 1998. Stratigraphy, depositional environment, and tectonic setting of the Upper Triassic to Middle Jurassic rocks of the Chilcotin Ranges, southwestern British Columbia. *Geological Survey of Canada Bulletin* 519, 58 p.